

# On The Pomeron at Large 't Hooft Coupling

Richard C. Brower\*, Matthew J. Strassler<sup>†</sup> and Chung-I Tan<sup>‡</sup>

E-mail: brower@bu.edu, strassler@physics.rutgers.edu, tan@het.brown.edu

October 25, 2018

## Abstract

We begin the process of unitarizing the Pomeron at large 't Hooft coupling. We do so first in the conformal regime, which applies to good accuracy to a number of real and toy problems in QCD. We rewrite the conformal Pomeron in the  $J$ -plane and transverse position space, and then work out the eikonal approximation to multiple Pomeron exchange. This is done in the context of a more general treatment of the complex  $J$ -plane and the geometric consequences of conformal invariance. The methods required are direct generalizations of our previous work on single Pomeron exchange and on multiple graviton exchange in AdS space, and should form a starting point for other investigations. We consider unitarity and saturation in the conformal regime, noting elastic and absorptive effects, and exploring where different processes dominate. Our methods extend to confining theories and we briefly consider the Pomeron kernel in this context. Though there is important model dependence that requires detailed consideration, the eikonal approximation indicates that the Froissart bound is generically both satisfied and saturated.

---

\*Physics Department, Boston University, Boston, MA 02215

<sup>†</sup>Department of Physics and Astronomy, Rutgers University, Piscataway, NJ 08854

<sup>‡</sup>Physics Department, Brown University, Providence, RI 02912

# Contents

<b>1</b>	<b>Introduction</b>	<b>4</b>
<b>2</b>	<b>Overview of Regge behavior in string theory</b>	<b>12</b>
2.1	Role of $J$ -plane singularities in flat space string theory . . . . .	12
2.2	An Aside on Fixed Poles . . . . .	15
2.3	The Pomeron in Impact Parameter Space . . . . .	17
<b>3</b>	<b>Eikonal Expansion of the AdS Pomeron</b>	<b>18</b>
3.1	Eikonal Graphs . . . . .	20
3.2	One-Loop Contribution: . . . . .	21
3.3	Feynman Rules and Eikonal Sum: . . . . .	24
<b>4</b>	<b>Conformal geometry at High Energies</b>	<b>25</b>
4.1	SL(2,C) Invariance of Pomeron kernel . . . . .	27
4.2	Pomeron Kernel at High Energies . . . . .	31
4.3	Connection with Graviton Exchange . . . . .	33
<b>5</b>	<b>Aspects of the Eikonal Representation</b>	<b>34</b>
5.1	Inelastic Production and $AdS$ . . . . .	35
5.2	Physical Consequences . . . . .	38
5.3	A Multi-Channel Interpretation . . . . .	41
5.4	Two-Pomeron Cut and Particle-Pomeron Amplitude . . . . .	43

5.5	Frozen String Bits in Flat Space . . . . .	45
<b>6</b>	<b>Unitarity, Confinement and Froissart Bounds</b>	<b>48</b>
6.1	Scattering in the Conformal Case . . . . .	49
6.2	Confinement and the Froissart Bound . . . . .	51
<b>7</b>	<b>Summary and Outlook</b>	<b>56</b>

# 1 Introduction

Recently there has been considerable effort — much of it using gauge/string duality — toward understanding high energy hadronic scattering in gauge theories. The conceptual and experimental importance of this problem is widely known, as is its difficulty. Here we take a step forward that will allow a number of interesting problems to be addressed.

The goal of this paper is to continue developing methods for implementing unitarity at finite 't Hooft coupling  $\lambda$ . In a wide regime of high energy scattering, Pomeron exchange is believed to be the dominant, universal process [1, 2, 3, 4, 5, 6, 7]. The Pomeron kernel with a leading  $J$ -plane singularity at  $j_0 > 1$  contributes to cross sections a growing power  $s^{j_0-1}$  (up to logarithms) in violation of unitarity. The eikonal approximation is an order-by-order summation of the leading  $(s^{j_0-1}/N^2)^n$  contribution to the  $n$ -Pomeron exchange process; here  $N$  is the number of colors. This approximation can only be valid in limited regimes, where the scattering angle is small. But understanding it represents a first step in satisfying the non-perturbative unitarization of high energy scattering [8, 9, 10].

A smaller step toward introducing unitarity corrections was made recently in the eikonal approximation for pure  $AdS_5$  gravity, [11, 12]; earlier related work includes [13, 14]. This limit represents taking  $\lambda \rightarrow \infty$  prior to considering large  $s$ . The power  $j_0$  is exactly 2 in this case.

Here we keep  $\lambda$  large but finite, and consider the richer question of Pomeron exchange with  $j_0 < 2$ , which is more relevant for QCD-like theories which have  $j_0$  considerably less than 2. We mainly present results for conformal field theories, but our results can easily be generalized to nonconformal theories, which we consider here only briefly. More difficult generalizations will involve including nonlinear effects and/or moving beyond the eikonal approximation.

The basic concepts involving high-energy hadron scattering in gauge/string duality have emerged in stages. It was shown in [15] that in exclusive hadron scattering, the dual string theory amplitudes, which in flat space are exponentially suppressed at wide angle, instead give the power laws that are expected in a gauge theory. Other related work includes [16, 17]. It was also argued that at large  $s$  and small  $t$  that the classic Regge form of the scattering amplitude, varying as  $s^{t/t_0}$ , is found in certain kinematic

regimes. Next, deep inelastic scattering was studied [18]. The moderate  $x$  regime was shown to be quite different from that of weak-coupling gauge theories due to much more rapid evolution of structure functions with  $q^2$ . The classical-twist-two operators develop large anomalous dimensions and (at finite but large  $N$ ) become subleading compared to double-trace, higher twist operators. At small  $x$ , by contrast, the physics is more similar to that of weak coupling, with a large growth in the structure functions controlled by Regge physics. The correct equations for the string-theory realization of the gauge-theory Pomeron were identified, along with the fact that the growth of the structure functions is controlled by a power  $j_0 - 1$  with  $j_0$  very close to, but less than, 2. After several interesting attempts using other methods [19, 20, 21, 22], it was demonstrated in [23] that the Pomeron equations of [18] could be easily solved and interpreted. The Pomeron was identified as a well-defined feature of the curved-space string theory. Its mathematical form in the conformal region of a gauge theory — the “hard” Pomeron — was shown to share many of the feature of the BFKL Pomeron for weak-coupling gauge theories. The Pomeron in the confining region was shown to have the features one would expect from QCD; running trajectories with bound states at integer  $j$ . Moreover, the “hard” and “soft” Pomerons were shown to be a single, unified object, as conjectured in [24, 25]. With this understanding of the Pomeron, any computation involving single-Pomeron exchange in a confining gauge theory can now, at least in principle, be carried out.

However, as we mentioned above, single-Pomeron exchange is only appropriate in limited regimes, since it violates unitarity at high energy. We now turn to the question of summing multiple Pomeron exchange where the scattering is sufficiently weak. As a preliminary, let us recall a result of [23]. In a conformal field theory, the Pomeron exchange kernel in the gauge theory can be represented in the dual string theory through a kernel  $\mathcal{K}$ , a function of  $s, t$  and two bulk coordinates  $z, z'$ .<sup>1</sup> This kernel is akin to a propagator for the Pomeron. At  $t = 0$  it has the very simple form,

$$\text{Im } \mathcal{K}(s, 0, z, z') \simeq \frac{s^{j_0}}{\sqrt{\pi \mathcal{D} \ln s}} e^{-(\ln z - \ln z')^2 / \mathcal{D} \ln s} \quad (1.2)$$

where  $j_0 = 2 - 2/\sqrt{\lambda}$  and  $\mathcal{D} = 2/\sqrt{\lambda}$ . This is strikingly similar to the weak BFKL

---

<sup>1</sup>Here the metric on the Poincare' patch of  $AdS_5$  is

$$ds^2 = \frac{R^2}{z^2} [\eta_{\mu\nu} dx^\mu dx^\nu + dz^2] \quad (1.1)$$

kernel [3, 4, 5],

$$\text{Im } \mathcal{K}(p_\perp, p'_\perp, s) \approx \frac{s^{j_0}}{\sqrt{\pi \mathcal{D} \ln s}} e^{-(\ln p'_\perp - \ln p_\perp)^2 / \mathcal{D} \ln s} \quad (1.3)$$

with  $j_0 = 1 + (4 \ln 2 / \pi) \alpha N$ ,  $\mathcal{D} = (14 \zeta(3) / \pi) \alpha N$ ,  $\alpha = g_{YM}^2 / 4\pi$ . This correspondence identifies diffusion in virtuality (or  $\log p_\perp^2$  for the off-shell gluons) with diffusion in the radial co-ordinate  $\log z^2$  in the dual  $AdS_5$  space.<sup>2</sup> For  $t \neq 0$  the form is somewhat more complicated, and is given below.

Our task will be to first reconsider the Pomeron kernel of [23] in the conformal regime. We will rewrite it in impact parameter space and in the  $J$ -plane, which greatly simplifies its form. In particular, as is the case for graviton exchange [11, 12], it involves an  $AdS_3$  scalar Green's function. We then use this answer to construct the eikonal approximation to the full amplitude, as we did in [12]. In doing so we include an infinite ladder of Pomeron exchanges, but neglect all non-linear Pomeron interactions. Of course this approximation is only valid in limited regimes, but we will not address the region of validity here. Within the regime in which it applies, the eikonal amplitude satisfies a form of bulk unitarity and exhibits both elastic and absorptive parts.

Our main results are the following. We begin with a conformal large- $N$  theory. For definiteness, consider adding a massive probe to such a theory, whose effects on the dynamics are subleading in  $1/N$ , such as a massive quark in the fundamental representation. Then consider  $2 \rightarrow 2$  high-energy scattering of gauge-neutral states associated to the probe (such as massive quarkonium states) at fixed  $s, t$ . The string description of this scattering depends not only on  $s, t$  but also on the bulk location  $z$  where the scattering occurs. In fact this is not enough; in general the scattering is not local, and could depend on the  $z$  locations of all four strings. However, there may be some regions of  $z, z'$ , and impact parameter  $b$  (where  $b \equiv x_\perp - x'_\perp$  is the distance in the two Minkowski space coordinates transverse to the motion), where the eikonal regime is valid. Let us separate the amplitude  $A_{2 \rightarrow 2}(s, t)$  into the region in position space variables where the eikonal approximation is valid — the “eikonal region”  $\mathcal{E}$  — and the regime where it is not. The contribution of the eikonal region to the amplitude — to which the amplitude

---

<sup>2</sup>In [23] the diffusion was taken with respect to  $\log z$ , or  $\log p_\perp$ , while standard conventions, to which we adhere in this paper, take diffusion in the variable  $\log z^2$  or  $\log p_\perp^2$ . Consequently the diffusion constant used here is normalized differently, compared to [23], by a factor of 4.

in the non-eikonal region, if any, must be added — is

$$- 2is \int_{\mathcal{E}} d^2b \, dz \, dz' \, P_{13}(z) P_{24}(z') e^{-ib^\perp q_\perp} \left[ e^{i\chi(s, x^\perp - x'^\perp, z, z')} - 1 \right] \quad (1.4)$$

(Here the scattering is of initial states 1, 2 to final states 3, 4.) The wave functions  $\Phi_i$  for the scattered states appear in pairs, evaluated at  $z$  for the right-moving states and at  $z'$  for the left-moving states:

$$P_{13}(z) = (z/R)^2 \sqrt{g(z)} \Phi_1(z) \Phi_3(z) \quad \text{and} \quad P_{24}(z') = (z'/R)^2 \sqrt{g(z')} \Phi_2(z') \Phi_4(z') \quad (1.5)$$

The eikonal kernel  $\chi$  is then a function of  $b, z, z'$  as well as  $s$ . This form of the amplitude is identical to that found for the eikonal approximation for graviton scattering in  $AdS_5$  space, except that now the function  $\chi$  is proportional not to the graviton propagator (projected onto  $AdS_3$ ) but to the Pomeron exchange kernel:

$$\chi(s, x^\perp - x'^\perp, z, z') = \frac{\kappa_5^2 R}{2(zz')^2 s} \mathcal{K}(s, x^\perp - x'^\perp, z, z') \quad (1.6)$$

where  $\kappa_5$  is the gravitational coupling constant in  $AdS_5$ . In the following, instead of  $\kappa_5^2$ , we will often use instead a dimensionless coupling  $g_0^2 = \kappa_5^2/R^3 \sim 1/N^2$ .

The kernel, as a function of  $s$  and transverse positions, is elegantly expressed through an inverse Mellin transform

$$\mathcal{K}(s, x^\perp - x'^\perp, z, z') = - \int \frac{dj}{2\pi i} \left( \frac{\widehat{s}^j + (-\widehat{s})^j}{\sin \pi j} \right) \mathcal{K}(j, x^\perp - x'^\perp, z, z') . \quad (1.7)$$

where

$$\widehat{s} \equiv zz' s \quad (1.8)$$

is dimensionless and

$$\mathcal{K}(j, x^\perp - x'^\perp, z, z') = (zz'/R^4) G_3(j, v) , \quad (1.9)$$

Here  $G_3(j, v)$  is the  $AdS_3$  Green's function which has a simple closed form,

$$G_3(j, v) = \frac{1}{4\pi} \frac{\left[ 1 + v + \sqrt{v(2+v)} \right]^{(2-\Delta_+(j))}}{\sqrt{v(2+v)}} . \quad (1.10)$$

It depends on the  $AdS_3$  chordal distance,

$$v = \frac{(x_\perp - x'_\perp)^2 + (z - z')^2}{2zz'} \quad (1.11)$$

and the  $AdS_3$  conformal dimension,  $\Delta_+(j) - 1$ , where

$$\Delta_+(j) = 2 + \sqrt{4 + 2\sqrt{\lambda}(j - 2)} = 2 + \sqrt{2\sqrt{\lambda}(j - j_0)} \quad (1.12)$$

sets the dimension  $\Delta$  as a function of spin  $j$  for the BFKL/DGLAP operators. The analytic continuation from DGLAP to BFKL operators has been discussed at weak coupling for some time [26, 27, 28, 29]. Recently, it was conjectured to be exact at weak coupling in  $\mathcal{N} = 4$  Yang-Mills theory [30]. The demonstration of this relationship in all large- $\lambda$  conformal theories, and the derivation of the formula (1.12), is given in section 3 of [23], where the existence of the single function  $\Delta_+(j)$  with  $j = j_0$  at  $\Delta = 2$  (the BFKL exponent) and  $j = 2$  at  $\Delta = 4$  (for the energy-momentum tensor, the first DGLAP operator) was demonstrated. For clarity, we reproduce Fig. 1 from [23] showing the essential form of this function for large and small  $\lambda$ .

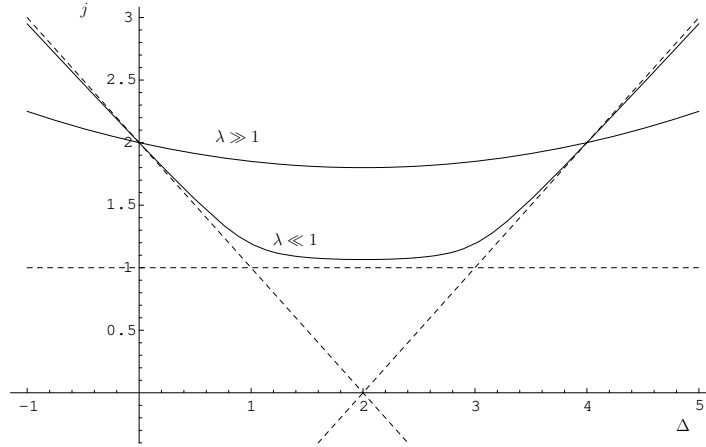


Figure 1: Schematic form of the  $\Delta - j$  relation for  $\lambda \ll 1$  and  $\lambda \gg 1$ . The dashed lines show the  $\lambda = 0$  DGLAP branch (slope 1), BFKL branch (slope 0), and inverted DGLAP branch (slope  $-1$ ). Note that the curves pass through the points  $(4, 2)$  and  $(0, 2)$  where the anomalous dimension must vanish. This curve is often plotted in terms of  $\Delta - j$  instead of  $\Delta$ , but this obscures the inversion symmetry  $\Delta \rightarrow 4 - \Delta$ .

The function  $G_3$  is shown in Fig. 2 for the Pomeron and graviton. Naturally it becomes large as  $v \rightarrow 0$ ; there the scattering is head-on in the bulk,  $\chi$  becomes large and



strongly varying, and the eikonal approximation will break down. Conversely at large  $v$  the eikonal approximation will be good; note this includes both large  $b$  compared to  $z$  and  $z'$  (where the scattered objects are at large impact parameter compared to their size) and at large  $z - z'$  for fixed  $z$  and  $z'$  (where their sizes are mismatched.)

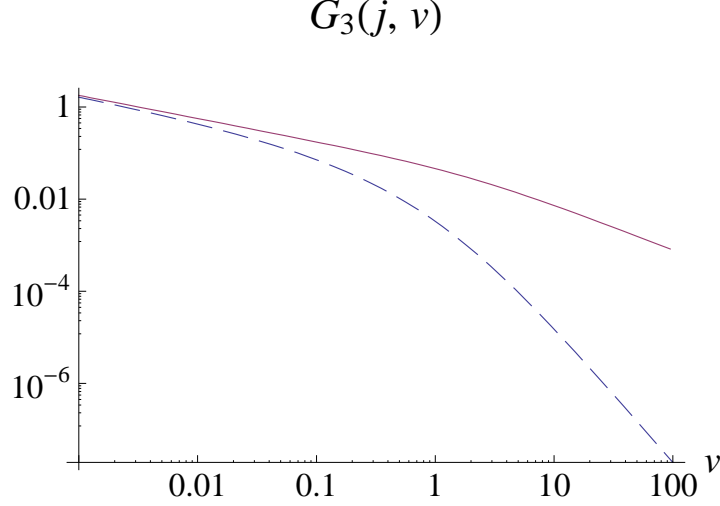


Figure 2: The function  $G_3(j, v)$  for  $j = j_0$  (the solid line for the Pomeron, with  $\Delta = 2$ ) and for  $j = 2$  (the dashed line for the graviton, with  $\Delta = 4$ ). Note  $G_3(j, v) \sim 1/\sqrt{v}$  for  $v \ll 1$  and  $\sim v^{1-\Delta+(j)}$  for  $v \gg 1$ . Thus the two functions have the same small- $v$  behavior, but the graviton falls off faster than the Pomeron.

We obtain the above form of the kernel as a Fourier transform of the conformal Pomeron

$$\mathcal{K}(j, x^\perp - x'^\perp, z, z') = \int \frac{d^2 q_\perp}{(2\pi)^2} e^{iq_\perp(x^\perp - x'^\perp)} \mathcal{K}(j, -q_\perp^2, z, z') \quad (1.13)$$

which was found in [23] to be

$$\mathcal{K}(j, t, z, z') = \frac{(zz')^2}{\pi^2 R^4} \int_{-\infty}^{\infty} d\nu (\nu \sinh \pi \nu) \frac{K_{i\nu}(qz) K_{-i\nu}(qz')}{\nu^2 + (2\sqrt{\lambda})(j - j_0)}. \quad (1.14)$$

This in turn is a Mellin transform of the imaginary part of the kernel as a function of  $s, t, z, z'$

$$\mathcal{K}(j, t, z, z') = \int_0^\infty d\hat{s} (\hat{s})^{-j-1} \text{Im } \mathcal{K}(s, t, z, z') \quad (1.15)$$

where again  $\hat{s} \equiv zz's$ . This strong coupling kernel [23] is a momentum space Green's function propagating in  $AdS_5$ , satisfying

$$[-z^5 \partial_z z^{-3} \partial_z - z^2 t + 2\sqrt{\lambda}(j-2)]\mathcal{K}(j, t, z, z') = R^{-4} z^5 \delta(z - z') . \quad (1.16)$$

It is also convenient to consider the spectral decomposition of the kernel with respect to  $t$ ,

$$\mathcal{K}(j, t, z, z') = \frac{(zz')^2}{2R^4} \int_0^\infty dk^2 \frac{J_{\tilde{\Delta}(j)}(zk) J_{\tilde{\Delta}(j)}(z'k)}{k^2 - t - i\epsilon} . \quad (1.17)$$

Here  $\tilde{\Delta}(j) \equiv \Delta_+(j) - 2$ .

Note finally that the full kernel, rather than just its imaginary part, can be reconstructed from the above expressions through

$$\mathcal{K}(s, t, z, z') = - \int \frac{dj}{2\pi i} \left( \frac{\hat{s}^j + (-\hat{s})^j}{\sin \pi j} \right) \mathcal{K}(j, t, z, z') . \quad (1.18)$$

Here, as in the flat-space string theory, the contour of integration is to the left of the poles at non-negative integers from the  $1/\sin \pi j$  factor and to the right of singularities of  $\mathcal{K}(j, t, z, z')$ .

After deriving these results in Sections 2 and 3, we discuss some interesting features of the single Pomeron exchange kernel in Sec. 4. We examine why the  $AdS_3$  Green's functions emerge in the form of the kernel, and the algebraic structure which underlies our formula for  $\Delta_+(j)$ . Next, we examine the high-energy behavior of the kernel as a function of  $s$  and  $b$ . As  $s \rightarrow \infty$ , with  $\lambda$  fixed, the Pomeron exchange is dominant, with

$$\chi \sim e^{i(1-j_0/2)\pi \hat{s}^{j_0-1}} G_3(j = j_0, v) \sim \frac{e^{i(1-j_0/2)\pi \hat{s}^{j_0-1}}}{\sqrt{v(2+v)}} \quad (s \rightarrow \infty) . \quad (1.19)$$

Note that the overall phase of the kernel is  $\exp[i(1-j_0/2)\pi]$ , independent of  $b, z, z'$ . However, at large fixed  $s$  and  $\lambda \rightarrow \infty$ , we recover the graviton exchange kernel of [11, 12],

$$\chi \sim \hat{s} G_3(j = 2, v) \sim \frac{\hat{s}}{[1 + v + \sqrt{v(2+v)}]^2 \sqrt{v(2+v)}} \quad (\lambda \rightarrow \infty) . \quad (1.20)$$

where  $G_3(2, v)$ , called  $G_3(v)$  in [12], is the dimensionless scalar propagator for a particle of mass  $\sqrt{3}/R$  in an  $AdS_3$  space of curvature radius  $R$ .

In Sec. 5 we turn to the features of the eikonal sum of multiple Pomeron exchanges. We discuss the physics of the non-trivial phase of the Pomeron and how the effects of

absorption are distributed over the bulk. Finally we reinterpret our results as those of a multi-channel eikonalization in the gauge-theory, consider how amplitudes for scattering a particle off a Pomeron are embedded in our results, and note some relations of our results with the string theory eikonal approximation [31, 32]. In particular we note that within the eikonal approximation, well known to be instantaneous in light-cone time, the scattering process acts on each bit of string independently, giving it its own eikonal phase.

Finally, in Sec. 6 we turn to the question of the saturation of the unitarity bound in various contexts.<sup>3</sup> We do this first for the bulk amplitude in a conformal theory. Next we consider briefly confining backgrounds, where the continuum spectrum in  $t$  at fixed spin- $j$  in Eq. (1.17) becomes a discrete sum over Regge trajectories. Our general methods are still applicable, though the technical difficulties and model-dependence are much greater, and our results are very limited. But we will argue from the eikonal approximation that the cross section appears generically to be proportional to  $(\log s)^2$ , both satisfying and saturating the Froissart bound.

---

<sup>3</sup>After the initial version of this paper was released, we noticed an error which invalidated some of the results of Sec. 6. Our corrected results in the conformal limit now turn out to be reasonably consistent with those of [33], which studied a different but related problem.

## 2 Overview of Regge behavior in string theory

String theory was invented largely to accommodate two phenomenological features of hadronic scattering related to Regge theory. The first is the existence of narrow resonances of higher and higher spin apparently lying on almost linear “trajectories” ( $j \sim m_j^2 + \text{const}$ ). The second is the Regge asymptotic limit for high energy scattering at fixed momentum transfer,

$$A(s, t) \sim s^{j_0 + \alpha' t} \quad (2.1)$$

where the trajectory function  $\alpha(t) = j_0 + \alpha' t$  is an extrapolation to  $t < 0$  of the linear relation  $\alpha(m_j^2) \simeq j$ , for  $j > 0$ . While this has proven to be an oversimplification, the proper relationship between singularities in the complex  $J$ -plane and high energy scattering was thoroughly investigated in this context. Indeed the multi-Regge behavior of the planar limit of flat space string theory with exactly linear trajectories provides an excellent pedagogical tool [34]. Consequently, before we extend this analysis to the recently understood Regge limit for the *AdS* dual to gauge theories, it is useful to review the arguments briefly in flat space. Moreover, as we note below, the general Regge framework introduced here is valid for any theory with sufficient convergence at high energies.

### 2.1 Role of $J$ -plane singularities in flat space string theory

In flat space, the tree-level string scattering amplitude has a meromorphic representation in the complex  $J$ -plane. The argument proceeds as follows. The high energy limit of tachyon scattering amplitude in the closed string sector is

$$A(s, t) = \int d^2 w |w|^{-2-\alpha(t)} |1-w|^{-2-\alpha(s)} \simeq 2\pi \frac{\Gamma(-\alpha(t)/2)}{\Gamma(1+\alpha(t)/2)} (e^{-i\pi/2} \alpha' s/4)^{\alpha(t)} \quad (2.2)$$

where  $\alpha(t) = 2 + \alpha' t/2$ . Since the original amplitude is crossing symmetric under the exchange  $u \leftrightarrow s$ , by virtue of  $s + t + u = 4m^2$ , Eq. (2.2) may be rewritten as,

$$A(s, t) \simeq -\beta(t) \left[ \frac{(-\alpha' s)^{\alpha(t)} + (-\alpha' u)^{\alpha(t)}}{\sin \pi \alpha(t)} \right] \quad (2.3)$$

to leading order at high energy,  $u \simeq -s$ , where the residue function<sup>4</sup> is  $\beta(t) = 2^{1-2\alpha(t)}\pi^2/\Gamma^2(1+\alpha/2)$ . This form is preferable, since the separation of the Regge contribution from the right-hand cut,  $(-\alpha's)^{\alpha(t)}$ , and the left-hand cut,  $(-\alpha'u)^{\alpha(t)}$ , obeys exact crossing symmetry. Moreover it can be shown that the full string amplitude  $A(s, t)$ , for large  $s$  away from the singularities on the real axis, is given by a sum of powers in  $s$ , without  $\log s$  corrections. This implies there are poles but not cuts, and hence meromorphy, in the complex  $J$ -plane.

Now let us return to the full amplitude to investigate the source of Regge behavior in terms of a complex  $J$ -plane. To relate this to the singularity structure of the complex  $J$ -plane requires two steps. First, the amplitude  $A(s, t)$  must be expressed as a dispersion relations over the right-hand ( $s > 0$ ) and left-hand ( $u > 0$ ) cuts (each of which is actually a series of delta functions in tree-level string theory). Second, each contribution to the imaginary parts associated to the cuts,  $A_s$  and  $A_u$ , must be separately transformed to the  $J$ -plane by

$$a_s(j, t) = \alpha' \int_0^\infty ds (\alpha's)^{-j-1} A_s(s, t), \quad (2.4)$$

and similarly for  $s \rightarrow u$  which for our crossing symmetric amplitude (2.2) implies  $a_u(j, t) = a_s(j, t)$ . Assuming, for some fixed  $t < 0$ , that  $A_s(s, t)$  is zero for  $s \in [0, s_0]$ , this is merely the Laplace transform in rapidity  $y = \ln(s/s_0)$ , giving an analytic function in  $j$ , defined initially for large enough  $\text{Re } j$ . The inverse Mellin transform is given by the contour integral,

$$A_s(s, t) = \int_{-i\infty+J_0}^{i\infty+J_0} \frac{dj}{2\pi i} (\alpha's)^j a_s(j, t), \quad (2.5)$$

choosing  $J_0$  to the right of all singularities. This inversion becomes clearer when viewed as a Fourier transform in  $\text{Im } j$ .

For  $t$  sufficiently negative such that  $A(s, t) = 0(1/|s|)$ , the dispersion relation for  $A(s, t)$ ,

$$A(s, t) = \int_0^\infty \frac{ds'}{\pi} \frac{A_s(s', t)}{s' - s - i\epsilon} + \int_0^\infty \frac{du'}{\pi} \frac{A_u(u', t)}{u' - u - i\epsilon} \quad (2.6)$$

allows us to reconstruct the full amplitude<sup>5</sup>

---

<sup>4</sup>For superstring graviton-graviton scattering, the residue  $\beta(t)$  has an extra factor of  $(\alpha(t)/2)^2$  to remove the tachyon [32]. In the open superstring sector the residue function has the simpler form  $\beta(t) = \alpha(t)/\Gamma[-\alpha(t)]$ .

<sup>5</sup>There are a variety of closely related transforms that define the  $J$ -plane with identical leading singu-

$$A(s, t) = - \int_{-i\infty+J_0}^{i\infty+J_0} \frac{dj}{2\pi i} \frac{(-\alpha's)^j a_s(j, t) + (-\alpha'u)^j a_u(j, t)}{\sin \pi j} \quad (2.7)$$

from the  $J$ -plane, where  $J_0 \simeq -1$ .

As one increases  $t$ , poles in  $j$  move to the right, and one must distort the contour to stay to the right of the singularity. Therefore, for general  $t$ , the contour should be to the left of the pole in  $1/\sin \pi j$  at  $j = 0$  and to the right of all singularities of  $a_s(j, t)$  and  $a_u(j, t)$ . For example, in an amplitude with vacuum quantum numbers in the  $t$ -channel, the leading pole is symmetric in  $s \leftrightarrow u$  interchange,

$$a_s(j, t) \simeq \frac{\beta(t)}{j - \alpha(t)} \quad , \quad a_u(j, t) \simeq \frac{\beta(t)}{j - \alpha(t)} \quad (2.8)$$

with positive charge conjugation  $C = +1$ . This leads to an amplitude,

$$A(s, t) \simeq - \frac{(1 + e^{-i\pi\alpha(t)})\beta(t)s^{\alpha(t)}}{\sin \pi\alpha(t)} \sim \Gamma[-\alpha(t)/2](e^{-i\pi/2}s)^{\alpha(t)} \quad (2.9)$$

with “positive signature” in the language of Regge theory. This effect of the leading trajectory reproduces the leading Regge approximation of our string amplitude, Eq. (2.3), for all  $t$ . Recall that in flat space closed string theory, the leading trajectory, which contains the zero mass graviton at  $j = 2$ , is the analogue of the Pomeron in gauge theory.

As an aside, we note that the leading negative charge conjugation ( $C = -1$ ) contribution is odd under  $s \leftrightarrow u$  interchange, giving a negative signature factor  $1 - e^{-i\pi\alpha(t)}$ . This contribution, in the context of weak coupling QCD, is the analogue of the BFKL Pomeron referred to as the “odderon” with an odd number of gluons exchanged in the  $t$ -channel. Both contributions are present in an oriented close string exchange process.

The generality of the definition of an analytic  $J$ -plane should be clear, in spite of our use of the planar closed string amplitude as a convenient pedagogical example. In general, complete knowledge of the  $J$ -plane singularity structure allows an *exact* representation of the full amplitude, if the amplitude has the required convergence for unsubtracted

---

larities. For example from the  $t$ -channel partial wave expansion, one is lead to the Sommerfeld-Watson transform,

$$A(s, t) = - \sum_{\eta=\pm 1} \int \frac{dj}{2\pi i} (2j+1) \frac{\eta + e^{-i\pi j}}{2 \sin \pi j} a^\eta(j, t) P(j, (s-u)/t) ,$$

where  $\eta$  is referred to as the signature:  $\eta = \pm 1$  for  $C = \pm 1$  exchange respectively.

dispersion relations at sufficiently negative  $t$ . Although Born terms in a perturbative field theory fail to satisfy this dispersion relation constraint, it is generally believed that full QCD does satisfy it, as well as a wide class of perturbative string theories, order by order in  $1/N$  or  $g_s$ . The flat-space critical superstring is the classic example, with an additional special feature that the tree-level amplitude exhibits meromorphy in *both* energy and the  $J$ -plane.<sup>6</sup> However, one lesson from gauge/string duality is that the gauge theory amplitudes dual to string theory in curved space need not show meromorphy in the  $J$ -plane, even in the planar limit; for instance this is illustrated by the BFKL singularity for the hard Pomeron in large- $N$  conformal field theories, where conformal invariance assures the presence of cuts in the  $J$ -plane. New branch cuts in the  $J$ -plane also show up, for both flat space string theory and gauge theory, at higher orders in  $g_s$  or  $1/N^2$ , and thus in an eikonal sum. Nevertheless, the knowledge of the  $J$ -plane singularities can in principle allow a full reconstruction of the full amplitudes.

## 2.2 An Aside on Fixed Poles

Here we address a general issue which is useful later, but can be omitted at a first reading. In Secs. 5.4 and 5.5 we will encounter integrals of the following type:

$$C_1(t) = \int_{-i\infty}^{i\infty} \frac{ds}{2\pi i} A(s, t) . \quad (2.10)$$

The integral (2.10) is defined when the amplitude vanishes at large  $s$  faster than  $1/|s|$ , thus satisfying an unsubtracted dispersion relation, Eq. (2.6). Such integrals will play a special role in our subsequent derivation of the eikonal approximation where  $A(s, t)$  is the crossing-even “particle-Pomeron” scattering amplitude, and this has been used extensively by Amati, Ciafaloni and Veneziano [32] in their discussion of eikonalization for closed (super)-strings in flat space. We will introduce the notation of a particle-

---

<sup>6</sup>The proof of meromorphy to the closed string tachyon scattering amplitude (2.2) is most easily done by using a modified  $J$ -plane defined by the Beta transform:

$$\tilde{a}_s(j, t) = \int_{-i\infty}^{i\infty} ds A(s, t) B(\alpha(s)/2 + 1, j + 1) = 2\pi \frac{\Gamma[j - \alpha(t)]\Gamma[j + 1]}{\Gamma[j + 1 - \alpha(t)/2]^2} .$$

It can be shown that this implies that the Mellin transform is an equivalent but less elegant meromorphic representation of the  $J$ -plane.

Pomeron amplitude in Sec. 3 and discuss its role for eikonalization further in Sec. 5.4 and 5.5. Here we point out how integral (2.10) arises from a  $J$ -plane perspective.

Because the amplitude is crossing even, its  $s$ -channel and  $u$ -channel discontinuities are equal,  $A_s = A_u$ . The integration path runs along the imaginary  $s$ -axis, crossing the real axis between the  $s$ - and  $u$ -cut. With the amplitude vanishing faster than  $1/|s|$ , one can distort the integration contour, e.g, one can integrate along the real axis, under the left-hand  $u$ -cut and over the right-hand  $s$ -cut. Alternatively, one can directly close the contour either to the right or to the left. When closing the contour, either to the left or to the right, one would pick up discontinuity across the respective cut, leading to

$$C_1(t) = (1/\pi) \int_0^\infty ds' A_s(s', t) = (1/\pi) \int_0^\infty du' A_u(u', t) \quad (2.11)$$

Historically, this contribution,  $C_1(t)$ , has been referred to as the  $j = -1$  “fixed-pole” residue.

To gain a better understanding on this contribution, consider the Regge representation for the full amplitude (2.7). As one pushes the contour to the left in  $j$ , the zero of the denominator  $\sin \pi j$  would appear to give rise to fixed powers  $s^{-N}$ ,  $N = 1, 2, \dots$ . However for the flat space closed string the leading term is  $s^{2+\alpha' t/2}$  so these contributions must be absent for sufficiently negative  $t$ . This implies zeroes in the numerator to cancel these poles. On the other hand we can also directly examine the amplitude with only a right-hand cut,

$$A_R(s, t) = \frac{1}{\pi} \int_0^\infty ds' \frac{A_s(s', t)}{s' - s} \rightarrow \beta(t) (-\alpha' s)^{\alpha(t)} - \frac{C_{1,s}(t)}{s} - \dots \quad (2.12)$$

with  $C_{1,s}(t) = (1/\pi) \int_0^\infty ds' A_s(s', t)$ , and similarly

$$A_L(u, t) = \frac{1}{\pi} \int_0^\infty du' \frac{A_u(u', t)}{u' - u} \rightarrow \beta(t) (-\alpha' u)^{\alpha(t)} - \frac{C_{1,u}(t)}{u} - \dots \quad (2.13)$$

with  $C_{1,u}(t) = (1/\pi) \int_0^\infty du' A_u(u', t)$ . For closed strings, crossing symmetry  $s \leftrightarrow u$  relates the left- and right-hand discontinuities, and it follows that  $C_{1,s}(t) = C_{1,u}(t) \equiv C_1(t)$ . Therefore, the fixed-pole residue is simply the coefficient of the fixed  $1/s$  and  $1/u$  contributions in the asymptotic expansion for  $A_R$  and  $A_L$  respectively. Note that the full amplitude,  $A(s, t) = A_R + A_L$ , does not contain the  $1/s$  term for  $s$  large. However, in Eq. (2.10), since the integration path runs between the left- and right-hand cuts, it cannot be distorted to infinity. As a consequence, the integral leads to a non-vanishing contribution, even if the full amplitude  $A(s, t)$  vanishes faster than  $1/|s|$ .



## 2.3 The Pomeron in Impact Parameter Space

The  $J$ -plane formalism can be applied to the Pomeron as understood in the work of Ref. [23]. For  $\mathcal{N} = 4$  SYM, or indeed any conformal theory dual to a string theory on  $AdS_5 \times M_5$ , the Pomeron propagator,  $\mathcal{K}(s, t, z, z')$  in Eq. (1.18), can be found at strong coupling. In Ref. [23], we have concentrated on the imaginary part of the full kernel,  $\text{Im}[\mathcal{K}]$ . In this section we transform the full kernel  $\mathcal{K}$  to the  $J$ -plane, and then to transverse position space. This leads to remarkable simplifications.

Just as done for the flat space string theory, it is useful to reconstruct the full amplitude through a  $J$ -plane representation. From the  $s$ -channel discontinuity,  $2i \text{Im } \mathcal{K}$ , one can obtain a  $J$ -plane amplitude via a Mellin transform. For the case of the  $AdS$  Pomeron, it is convenient to define the Mellin transform with respect to

$$\widehat{s} = zz's, \quad (2.14)$$

where the dimensionless variable,  $\widehat{s}$ , is  $R^2$  times the proper center-of-mass energy squared. Starting from the imaginary part of  $\mathcal{K}(s, t, z, z')$ , obtained in [23], we can find the kernel in the  $J$ -plane,  $\mathcal{K}(j, t, z, z')$ , using Eq. (1.15). The strong coupling kernel in the  $J$ -plane,  $\mathcal{K}(j, t, z, z')$ , is a momentum space Green's function propagating in  $AdS_5$

$$[-z^5 \partial_z z^{-3} \partial_z - z^2 t + 2\sqrt{\lambda}(j-2)]\mathcal{K}(j, t, z, z') = R^{-4} z^5 \delta(z - z') \quad (2.15)$$

We can always reconstruct the full amplitude,  $\mathcal{K}(s, t, z, z')$ , using an inverse Mellin transform, Eq. (1.18). As in the flat-space string theory, the contour of integration must be to the left of the poles at positive integers from the  $1/\sin \pi j$  factor, and to the right of singularities of  $\mathcal{K}(j, t, z, z')$ .

From a spectral analysis for Eq. (2.15) in momentum space, following [23], we can obtain

$$\mathcal{K}(j, t, z, z') = \frac{(zz')^2}{\pi^2 R^4} \int_{-\infty}^{\infty} d\nu (\nu \sinh \pi \nu) \frac{K_{i\nu}(qz) K_{-i\nu}(qz')}{\nu^2 + (2\sqrt{\lambda})(j - j_0)}, \quad (2.16)$$

where  $j_0 = 2 - 2/\sqrt{\lambda}$ . This expression masks the simplicity of the conformal invariance, but illustrates that the  $J$ -plane spectrum consists of only a continuum, with a square-root branch point at  $j_0$ , i.e.,  $\mathcal{K}(j, t, z, z') \sim \sqrt{j - j_0}$ , where  $j_0$  is the location of BFKL branch point in the strong coupling. Although the location of the BFKL cut is  $t$ -independent, the discontinuity depends on  $t$ , for fixed  $z, z'$ . Also, in the limit  $t \rightarrow 0$ , with  $z, z'$  fixed, the

nature of the singularity changes: as demonstrated in Ref. [23],  $\mathcal{K}(j, 0, z, z') \sim 1/\sqrt{j - j_0}$ , which leads to an asymptotic behavior  $\tilde{s}^{j_0}/\log^{1/2} \tilde{s}$ , as indicated in Eq. (1.2).

Now, in preparation for the eikonal application, we move to transverse impact parameter space:  $x^\perp = (x^1, x^2)$ . Introducing the conjugate transverse momentum vector,  $q_\perp = (q_1, q_2)$  where  $t = -q_\perp^2$ , we obtain from Eq. (1.14)

$$\mathcal{K}(j, x^\perp - x'^\perp, z, z') = \int \frac{d^2 q_\perp}{(2\pi)^2} e^{iq_\perp(x^\perp - x'^\perp)} \mathcal{K}(j, -q_\perp^2, z, z') = \left( \frac{zz'}{R^4} \right) G_3(j, v), \quad (2.17)$$

where  $G_3(j, v)$  is defined in Eq. (1.10). This elegant expression deserves an explanation, which we postpone to Sec 4, in order to move swiftly to the eikonal expansion.

Now using the impact-parameter-space version of Eq. (1.18), namely Eq. (1.7), we can obtain  $\mathcal{K}(s, x^\perp - x'^\perp, z, z')$ , which is the kernel in the form needed for the eikonal calculation. We will return in Section 4 to examine its high energy behavior more carefully. Here we merely remark on its phase. Due to the BFKL branch point,

$$\mathcal{K}(s, x^\perp - x'^\perp, z, z') \sim -\frac{\widehat{s}^{j_0} + (-\widehat{s})^{j_0}}{\sin \pi j_0} = -\left( \frac{e^{-\pi j_0/2}}{\sin \pi j_0/2} \right) \widehat{s}^{j_0} \quad (2.18)$$

up to logarithmic corrections.<sup>7</sup>

### 3 Eikonal Expansion of the AdS Pomeron

We now turn to the problem of the eikonal summation of multiple Regge exchange graphs for the  $AdS_5$  strong coupling Pomeron. It is easy to infer the answer by comparison with two simpler examples: the well known eikonalization of a single Regge-pole exchange in the single 2-to-2 elastic unitarity approximation, and the recent eikonal formula [12, 11] for graviton exchange at infinite coupling in  $AdS_5$ . The first introduces a non-trivial phase in the Regge exchange kernel. The second brings into play the radial co-ordinate

---

<sup>7</sup>The expression second from the right, though less compact than the rightmost expression, will be used below, in order to continue to exhibit the connection between the Regge phase and the  $s$ - and  $u$ -channel discontinuities. Therefore the coefficient of  $s^{j_0}$  is complex, and independent of the coordinates  $b, z, z'$ , in the region where the Regge form of amplitude is applicable. Here,  $(-s)^{j_0}$  and  $s^{j_0}$  separately represent asymptotic behavior for amplitudes with  $s$ - and  $u$ -channel discontinuities. The fact that the Pomeron kernel is complex will be important when we discuss  $s$ -channel unitarity in Section 5.

in  $AdS_5$ , which combines with the Minkowski-space impact parameter to form an  $AdS_3$  transverse space, a point we return to in section 4. Here and below, to simplify formulas, we temporarily set the  $AdS$  curvature radius  $R$  to 1.

For pedagogical reasons we will begin by presenting the form of the eikonal representation in  $AdS_5$  before providing its derivation and a description of its properties. Also we will make a comparison in Sec. 5.5 with a third example, namely the eikonal approximation for the flat space superstring amplitude, due to Amati, Ciafaloni and Veneziano. Together these examples provide a general intuitive picture to guide further advances beyond the eikonal approximation.

The standard eikonal formula takes the classic form,

$$A(s, t) = -2is \int d^2b e^{-ib^\perp q_\perp} \left[ e^{i\chi(s, b^\perp)} - 1 \right], \quad (3.1)$$

where  $t = -q_\perp^2$ . For a single Regge pole exchange, as for the Pomeron,  $\chi(s, b^\perp)$  is the Fourier transform to impact parameter space of the elastic amplitude in the one-Reggeon exchange approximation,

$$\chi(s, b^\perp) = \frac{1}{2s} \int \frac{d^2q_\perp}{(2\pi)^2} e^{ib^\perp q_\perp} A^{(1)}(s, t), \quad (3.2)$$

with  $A^{(1)}(s, t) = -[(e^{-i\pi\alpha(t)} \pm 1)/\sin \pi\alpha(t)]\beta(t)s^{\alpha(t)}$ . (See also Eq. (2.2) for the closed string form of  $A^{(1)}(s, t)$ .) This is the leading contribution to the sum of graphs depicted in Fig. 3 below. Let us compare this with our result for the eikonalization of the  $AdS_5$  graviton of Ref. [12]

$$A_{2 \rightarrow 2}(s, t) \simeq -2is \int d^2b e^{-ib^\perp q_\perp} \int dz dz' P_{13}(z) P_{24}(z') \left[ e^{i\chi(s, b^\perp, z, z')} - 1 \right] \quad (3.3)$$

where  $b = x^\perp - x'^\perp$  due to translational invariance. The salient new features relative to the above four-dimensional expressions are the new transverse co-ordinate for the fifth dimension in  $AdS_5$  and the product of wave functions for right-moving ( $1 \rightarrow 3$ ) and left-moving ( $2 \rightarrow 4$ ) states,

$$P_{13}(z) = (z/R)^2 \sqrt{g(z)} \Phi_1(z) \Phi_3(z) \quad \text{and} \quad P_{24}(z) = (z'/R)^2 \sqrt{g(z')} \Phi_2(z') \Phi_4(z') \quad (3.4)$$

The obvious (and correct) guess for the eikonalization of  $AdS_5$  Pomeron is to simply use the appropriate  $AdS_3$  kernel for this exchange as presented above in Sec. 1,

$$\chi(s, x^\perp - x'^\perp, z, z') = \frac{g_0^2 R^4}{2(zz')^2 s} \mathcal{K}(s, x^\perp - x'^\perp, z, z') \quad (3.5)$$

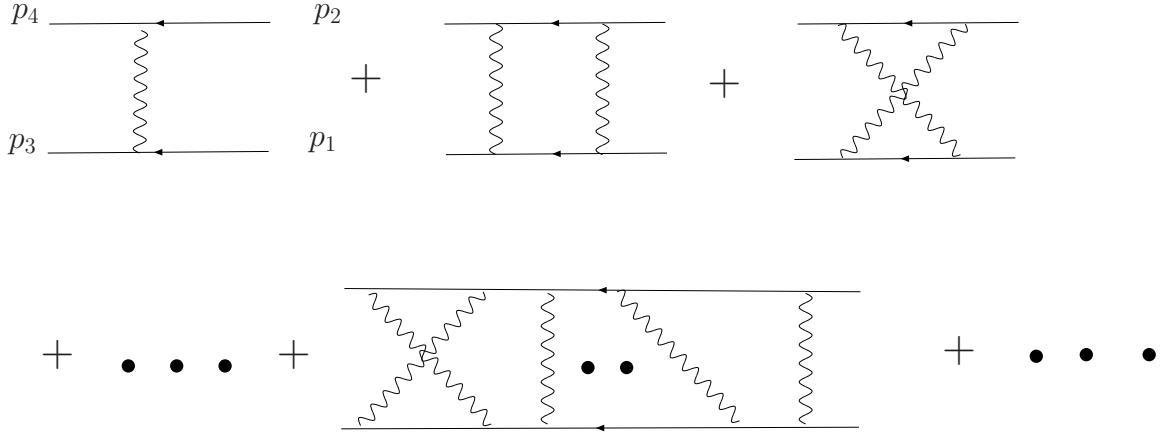


Figure 3: Ladder and crossed ladder diagrams contributing to the eikonal approximation in the high energy limit.

where  $g_0^2 = \kappa_5^2/R^3$ . This is a natural generalization of our earlier result for  $AdS$  graviton exchange, whose kernel can be obtained from the same  $J$ -plane analysis by taking the limit  $\lambda \rightarrow \infty$ , as explained in Sec. 4.3.

### 3.1 Eikonal Graphs

In Ref. [12], we have considered the high energy limit of a class of Witten diagrams, illustrated in Fig. 3, where we choose scalar fields for the external lines along two sides of the ladder and gravitons for the exchanged rungs between these two sides. The sum includes all possible  $AdS$  graviton exchanges, crossed and uncrossed. The treatment of the eikonal sum for conformal Pomeron exchanges follows exactly as that for the  $AdS$  graviton. The only new ingredient is to replace each  $AdS$  graviton propagator by a conformal Pomeron propagator,  $\mathcal{K}(s, x^\perp - x'^\perp, z, z')$ , Eq. (1.7). Because we work in to leading order in strong coupling, we can again treat the two scattered particles — the sides of the ladder — by using an  $AdS_5$  scalar propagator, as was done in Ref. [12]. String excitations on the sides of the ladder enter at higher order in  $1/\sqrt{\lambda}$ , and can be ignored for our current purposes.

Most of the needed analysis was done in Ref. [12] and will not be repeated here. We only outline briefly how the eikonal sum can be carried out, though we will spell out

explicitly the Feynman rules for the eikonal graphs. For a 2-to-2 amplitude,  $1 + 2 \rightarrow 3 + 4$ , let us denote the longitudinal momenta by  $p_1^\pm + p_2^\pm \rightarrow p_3^\pm + p_4^\pm$ , with an all-incoming convention. We will work in a transverse coordinate basis, using  $p^+, p^-, x^\perp, z$  as coordinates. In this representation, after stripping away a wave function for each external particle,  $\Phi_i(z)e^{-ip^\perp x^\perp}$ , we will be left to calculate an amputated amplitude,  $\mathcal{A}(p_i^\pm, x_i^\perp, z_i)$ , as a perturbative sum of diagrams illustrated in Fig. 3.

In the high-energy near-forward limit,  $p_1^+ \simeq -p_3^+$  and  $p_2^- \simeq -p_4^-$  are large, with  $q^\pm = p_1^\pm + p_3^\pm = -(p_2^\pm + p_4^\pm) = 0(1/\sqrt{p_1^+ p_2^-})$ . Therefore,  $\mathcal{A}$  depends on longitudinal momenta only through  $s \simeq 2p_1^+ p_2^-$ , and we can simply express the amplitude as  $\mathcal{A}(s, x_i^\perp, z_i)$ . It is in fact useful to view this as matrix elements of an operator,  $\mathbf{A}$ , in transverse coordinate basis,

$$\mathcal{A}(s, x_i^\perp, z_i) = \langle x_3, z_3, x_4, z_4 | \mathbf{A} | x_1, z_1, x_2, z_2 \rangle = \langle 3, 4 | \mathbf{A} | 1, 2 \rangle, \quad (3.6)$$

with states normalized by

$$\langle 3, 4 | 1, 2 \rangle = [\delta^2(x_1^\perp - x_3^\perp)\delta(z_1 - z_3)/\sqrt{g_1}][\delta^2(x_2^\perp - x_4^\perp)\delta(z_2 - z_4)/\sqrt{g_2}]. \quad (3.7)$$

Perturbative diagrams can be organized by the number of Pomeron propagators exchanged.

Let us begin by examining the simplest diagram – the tree graph. Since this involves a single Pomeron propagator, the amputated amplitude in transverse coordinate representation is given by

$$\mathcal{A}^{(1)}(s, x_i^\perp, z_i) = 2 \left( \frac{z_1 z_2}{R^2} \right)^2 s \chi(s, x_1^\perp - x_2^\perp, z_1, z_2) \langle 3, 4 | 1, 2 \rangle. \quad (3.8)$$

The  $\langle 3, 4 | 1, 2 \rangle$  factor is supplied so as to reproduce the single Pomeron exchange contribution obtained in Sec. 2. Note that  $\mathcal{A}^{(1)}$  is diagonal in the transverse coordinate basis.

## 3.2 One-Loop Contribution:

Before presenting the result for general graphs with  $n$  Pomeron exchanges, we first consider the one-loop contribution, illustrated in Fig. 4. There are two independent diagrams, which are depicted in the upper half of Fig. 4. For reason to be clarified shortly, the sum of these two diagrams can be combined as a product of two “Pomeron-particle” amplitudes,

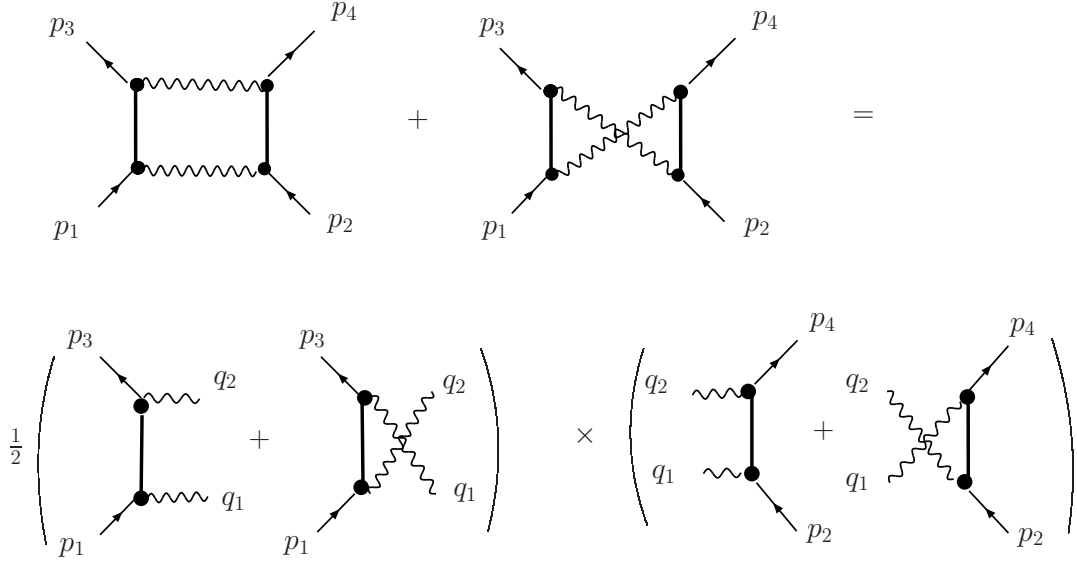


Figure 4: Sum of box and crossed box diagrams is factorized with combinatoric weight  $1/2!$ .

$A_{13}$  and  $A_{24}$ , (see Fig. 5), connecting through two Pomeron kernels, as schematically represented by the lower half of Fig. 4. However, this leads to an over-counting, and a factor of  $1/2!$  is supplied.

It is important to appreciate the assumptions made in evaluating the one-loop contribution in the high energy eikonal approximation. We assume that it is proper to factorize the contribution into exchange Pomeron kernels for the rungs of the ladder and 2-2 Pomeron-particle scattering amplitudes  $A_{13}$  and  $A_{24}$  on the sides. In an elementary field theory, e.g., the eikonal sum for exchanging conformal gravitons, this is a trivial combinatoric fact as illustrated in Fig. 4. In string theory this is an assumption on the high energy limit of the one loop diagram, only proven for the flat space superstring to date [32]. However we should note that the existence of these Pomeron-particle amplitudes is supported by the observation in Ref. [23] that the Pomeron vertex is a proper on-shell vertex operator with conformal weight  $(1,1)$  in string theory, both in flat space and to leading order in an  $AdS$  background.

The Pomeron-particle elastic-scattering amplitude in the planar limit can be expressed through a dispersion relation as a sum of  $s$ -channel and  $u$ -channel closed string

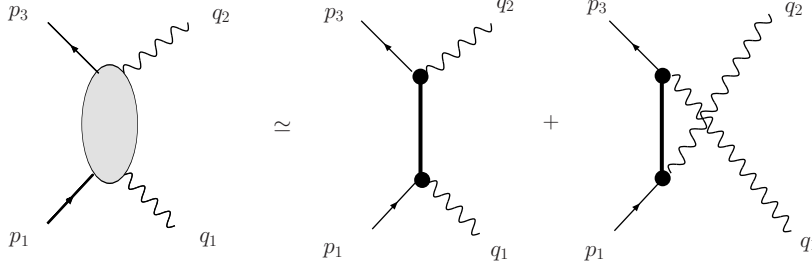


Figure 5: Reggeon particle scattering amplitude in the planar approximation,  $A_{13}(M^2, t)$ , with  $t = (q_1 + q_2)^2$  and  $M^2 = (p_1 + q_1)^2$ .

exchanges (see Fig. 5). As we noted, at the leading order in strong coupling, we can represent this amplitude using the scalar propagator,  $G_5(2p^+p^-, x^\perp - x'^\perp, z, z')$ , in the bulk of  $AdS_5$ . This scalar propagator is the solution of Eq. (2.15) at  $j = 2$ , but normalized without a factor of  $R^{-4}$ , so it has the scaling dimension of  $(\text{length})^2$ . Again we use a transverse coordinate representation, expressing  $G_5$  in terms of  $p^\pm$  and  $x^\perp - x'^\perp$ . A useful spectral representation for  $G_5$  is

$$G_5(2p^+p^-, x^\perp - x'^\perp, z, z') = \frac{(zz')^2}{2} \int \frac{d^2p^\perp}{(2\pi)^2} e^{ip^\perp(x^\perp - x'^\perp)} \int_0^\infty dk^2 \frac{J_2(zk)J_2(z'k)}{k^2 + p^{\perp 2} - 2p^+p^- - i\epsilon}. \quad (3.9)$$

Following a by-now standard procedure [32, 35, 36], the total one-loop contribution at high energies can be expressed as,

$$\begin{aligned} \mathcal{A}^{(2)}(p_i^\pm, x_i^\perp, z_i) &= -i \frac{i^4 g_0^4}{2!} \int dq_1 dq_2 A_{13}(p_1^\pm, q_1^\pm, x_3^\perp - x_1^\perp, z_3, z_1) \mathcal{K}(s, x_1^\perp - x_2^\perp, z_1, z_2) \\ &\quad \mathcal{K}(s, x_3^\perp - x_4^\perp, z_3, z_4) A_{24}((p_2^\pm, q_2^\pm, x_4^\perp - x_2^\perp, z_4, z_2) \end{aligned} \quad (3.10)$$

where the phase space is written symmetrically as

$$\int dq_1 dq_2 \equiv \int \frac{dq_1^+ dq_1^-}{2\pi} \frac{dq_2^+ dq_2^-}{2\pi} \delta(q_1^+ + q_2^+ - q^+) \delta(q_1^- + q_2^- - q^-) \quad (3.11)$$

with  $q_1^\pm$  and  $q_2^\pm$  the longitudinal momentum associated with the two Pomeron exchanges.

As emphasized earlier, in the near forward limit, we have  $q^\pm \simeq 0$ , so in fact,  $q_1^\pm = -q_2^\pm$ . The structure for  $\mathcal{A}^{(2)}$  is identical to that for the exchange of two  $AdS$  gravitons in Ref. [12], with conformal Pomeron propagators replacing  $AdS$  graviton propagators. As noted earlier, the Pomeron propagators,  $\mathcal{K}$ , are independent of longitudinal momenta,  $q_i^\pm$  and can be taken outside of the integrals.

In Eq. (3.10),  $A_{13}$  and  $A_{24}$  are Pomeron-particle amplitudes mentioned earlier and, in strong coupling, each reduces to a sum of two scalar propagators  $G_5$ , reflecting direct and crossed exchanges along each side of the ladder, e.g.,

$$A_{13}(p_1^\pm, q_1^\pm, x_3^\perp - x_1^\perp, z_3, z_1) = \frac{1}{R^3} [G_5(p_1^\pm, q_1^\pm, x_3^\perp - x_1^\perp, z_3, z_1) + G_5(p_1^\pm, q_2^\pm, x_3^\perp - x_1^\perp, z_3, z_1)] \quad (3.12)$$

At high energy, ( $p_1^+$  and  $p_2^-$  large with  $p_1^- \sim 0$  and  $p_2^+ \sim 0$ ),  $A_{13}$  depends only on the integration variable  $q_1^-$  through the combination  $p_1^+ q_1^-$  and  $A_{24}$  only on  $q_1^+$  through  $p_2^- q_1^+$ , so that integrals  $\int dq_1^- A_{13}$  and  $\int q_1^+ A_{24}$  can be carried out independently. This “left-right” factorization is one of the key properties which allows eikonalization to proceed. From the spectral representation for  $G_5$ , and the completeness relation, one arrives at a remarkably simple result,

$$\left( \int \frac{dq_1^-}{2\pi i} A_{13} \right) \left( \int \frac{dq_1^+}{2\pi i} A_{24} \right) = (1/2sR^6) \delta^2(x_1^\perp - x_3^\perp) z_1^3 \delta(z_1 - z_3) \delta^2(x_2^\perp - x_4^\perp) z_2^3 \delta(z_2 - z_4) \quad (3.13)$$

Putting all terms together, we obtain

$$\begin{aligned} \mathcal{A}^{(2)}(s, x_i^\perp, z_i) &= \langle 3, 4 | \mathcal{A}^{(2)} | 1, 2 \rangle \\ &\simeq -2i(zz'/R^2)^2 s \frac{1}{2!} [i\chi(s, x^\perp - x'^\perp, z, z')]^2 \langle 3, 4 | 1, 2 \rangle \end{aligned} \quad (3.14)$$

This has been discussed carefully in Ref. [12], to which the reader is referred for more details.

### 3.3 Feynman Rules and Eikonal Sum:

Feynman rules for higher order eikonal graphs can be written down fairly simply. In  $n$ th order, there are  $n$   $AdS_3$  vertices on each side to the ladder. Each vertex on one side is connected to one and only one vertex on the opposite side by a conformal Pomeron propagator; there are  $n!$  such distinct graphs. The Feynman rules are:

1. A Pomeron kernel,  $\mathcal{K}(s, x^\perp - x'^\perp, z, z')$ , for each rung across the ladder,
2. An  $AdS_5$  scalar propagator,  $R^{-3}G_5(2p^+p^-, x_{i+1}^\perp - x_i^\perp, z_{i+1}, z_i)$ , connecting each adjacent vertices along the side of the ladder.



3. A factor of  $g_0$  for each vertex, and a factor of  $i$  for each propagator.
4. An overall factor of  $-i$ .

To calculate the  $n$ th order amputated amplitude,  $\mathcal{A}^{(n)}(s, x_i^\perp, z_i)$ , one integrates over all loop longitudinal momenta, with momentum conservation at each vertex. One also integrates all internal transverse coordinates, except for  $(x_i^\perp, z_i)$ ,  $i = 1, 2, 3, 4$ , to which external momentum  $p_i^\pm$  are attached. Summing over  $n$  leads to the total amputated amplitude  $\mathcal{A}(s, x_i^\perp, z_i)$ . To obtain the momentum space scattering amplitude,  $A(s, t)$  from  $\mathcal{A}(s, x_i^\perp, z_i)$ , one supplies external wave functions,  $e^{-iq_i^\perp x_i^\perp} \Phi(z_i)$ , and integrates over the transverse coordinates.

It suffices to point out that the evaluation for higher order contributions proceeds also as has been done for *AdS* graviton exchange. As stressed in Ref. [12], for each order in a perturbative eikonal sum, one can again demonstrate the feature of “zero transverse deflection,” and the amplitudes becomes diagonal in the transverse basis. To be precise, we find that the amputated amplitude, at each order, takes on the form

$$\begin{aligned}
\mathcal{A}^{(n)}(s, x_i^\perp, z_i) &= \langle 3, 4 | \mathcal{A}^{(n)} | 1, 2 \rangle \\
&\simeq -2i(zz')^2 s \frac{1}{n!} [i\chi(s, x^\perp - x'^\perp, z, z')]^n \langle 3, 4 | 1, 2 \rangle
\end{aligned}
\tag{3.15}$$

Summing over  $n = 1, 2, \dots$ , leads to the desired eikonal representation. After integrating out  $(x_i^\perp, z_i)$ ,  $i = 1, \dots, 4$ , and removing a two-dimensional delta-function associated with the center-of-mass motion in impact space, we arrive at the eikonal representation, Eq. (3.3), with the eikonal given by Eq. (3.5), as promised.

## 4 Conformal geometry at High Energies

We now turn to a more detailed consideration of the Pomeron kernel with an emphasis on the consequences of conformal invariance for high energy amplitudes. This not only explains the simple properties of the kernel, it also gives a geometrical picture of Regge scattering in *AdS* space.

To see intuitively how this picture comes about let us reconsider the Regge limit for a general  $n$ -particle scattering amplitude:  $A(p_1, p_2, \dots p_n)$ . As argued in Ref. [23], the general Regge exchange corresponds to a large rapidity gap separating the  $n$  particles into two sets: the right movers and left movers, with large  $p_r^+ = (p_r^0 + p_r^3)/\sqrt{2}$  and large  $p_\ell^- = (p_\ell^0 - p_\ell^3)/\sqrt{2}$  momenta respectively. The Pomeron exchange kernel is obtained by applying this limit to the leading diagram, in the  $1/N$  expansion, that carries vacuum quantum numbers in the  $t$ -channel. The Pomeron exchange graph in string theory is a cylinder, a  $t$ -channel closed string.

The rapidity gaps,  $\ln(p_r^+ p_\ell^-)$ , between any right- and left-moving particles are all  $O(\log s)$ , i.e., a large Lorentz boost,  $\exp[yM_{+-}]$ , with  $y \sim \log s$ , is required to switch from the frame comoving with the left movers to the frame comoving with the right movers. The  $J$ -plane is conjugate to rapidity, and as such is identified with the eigenvalue of the Lorentz boost generator  $M_{+-}$ . In the context of the AdS/CFT correspondence, it is illuminating to consider the boost operator relative to the full  $O(4, 2)$  conformal group, which are represented as isometries of  $AdS_5$ .

The conformal group  $O(4, 2)$  has 15 generators:  $P_\mu, M_{\mu\nu}, D, K_\mu$ . In terms of transformations on light-cone variables, there are two interesting 6 parameter subgroups: The first is the well known collinear group  $SL_L(2, R) \times SL_R(2, R)$  used in DGLAP, with generators

$$SL_L(2, R), SL_R(2, R) \quad \text{generators:} \quad D \pm M_{+-}, P_\pm, K_\mp, \quad (4.1)$$

which corresponds in the dual  $AdS_5$  bulk to isometries of the Minkowski  $AdS_3$  light-cone sub-manifold. The second is  $SL(2, C)$  (or Möbius invariance used in solving the weak coupling BFKL equations) with generators

$$SL(2, C) \quad \text{generators:} \quad iD \pm M_{12}, P_1 \pm iP_2, K_1 \mp iK_2, \quad (4.2)$$

corresponding to the isometries of the Euclidean (transverse)  $AdS_3$  subspace of  $AdS_5$ ; Euclidean  $AdS_3$  is the hyperbolic space  $H_3$ . Indeed  $SL(2, C)$  is the subgroup generated by all elements of the conformal group that commute with the boost operator,  $M_{+-}$  and as such plays the same role as the little group which commutes with the energy operator  $P_0$ . For example we note that the BFKL Pomeron kernel in the  $J$ -plane is a solution of an  $SL(2, C)$  invariant operator equation in both strong and weak coupling. Very likely this is a generic property for the Pomeron in all conformal gauge theories.

## 4.1 $SL(2,C)$ Invariance of Pomeron kernel

In high energy small-angle scattering, the problem separates into the longitudinal and transverse directions relative to the momentum direction of the incoming particles. The transverse subspace of  $AdS_5$  is  $AdS_3$ . We shall show that this is reflected in the co-ordinate representation for the Pomeron kernel of Ref. [23] as a bulk-to-bulk scalar propagator in the transverse Euclidean  $AdS_3$  with  $SL(2,C)$  isometries.

Recall that our conformal strong coupling Pomeron kernel (or “Reggized  $AdS_5$  graviton”) from Ref. [23] was written in momentum space as an  $AdS_5$  Green’s function,

$$[-z^5 \partial_z z^{-3} \partial_z - z^2 t + 2\sqrt{\lambda}(j-2)]\mathcal{K}(j, t, z, z') = R^{-4} z^5 \delta(z - z') . \quad (4.3)$$

with  $AdS_5$  mass squared  $2\sqrt{\lambda}(j-2)/R^2$ . However in practice one can use an impact parameter representation in which the Pomeron kernel can be re-expressed in terms of an  $AdS_3$  Green’s function,

$$\mathcal{K}(j, x^\perp - x'^\perp, z, z') = \left( \frac{zz'}{R^4} \right) G_3(j, v) , \quad (4.4)$$

as noted in the Introduction. Here  $G_3(j, v)$  has a simple closed-form expression (1.10) as a function of the  $AdS_3$  chordal distance,  $v = [(x_\perp - x'_\perp)^2 + (z - z')^2]/2zz'$ , that greatly simplified our subsequent analysis of multi-Pomeron exchange. Let us explain this “accident” in more geometrical terms.

The singularities in the  $J$ -plane must be determined by the eigenvalues of the boost operator, which for our  $AdS$  Pomeron<sup>8</sup> is approximated by  $M_{+-} = 2 - H_{+-}/(2\sqrt{\lambda}) + O(1/\lambda)$  to leading order in strong coupling. In this context we find that the  $AdS_3$  Green’s function for the Pomeron obeys the differential equation,

$$[H_{+-} + 2\sqrt{\lambda}(j-2)]G_3(j, x_\perp - x'_\perp, z, z') = z^3 \delta(z - z') \delta^2(x_\perp - x'_\perp) \quad (4.5)$$

for the boost operator, where

$$H_{+-} = -z^3 \partial_z z^{-1} \partial_z - z^2 \nabla_{x_\perp}^2 + 3 . \quad (4.6)$$

---

<sup>8</sup>In Ref. [23] the eigenvalue condition  $M_{+-} = j$  was also identified with the on-shell condition for the world sheet dilatation:  $L_0 + \bar{L}_0 - 2 = 0$ . Here we are concerned with the target space isometries.

To relate this to our earlier expression [23] for the Pomeron co-ordinate space kernel as an  $AdS_5$  Green's function,

$$[-z^5 \partial_z z^{-3} \partial_z + z^2 (\partial_+ \partial_- - \nabla_\perp^2) + 2\sqrt{\lambda}(j-2)]G_5(j, x-x', z, z') = z^5 \delta(z-z') \delta^4(x-x') , \quad (4.7)$$

we need to recognize that in the Regge limit this exchange kernel couples exclusively to nearly light-like left- and right-moving sources. Consequently to compute the high energy amplitude, we only need the  $AdS_5$  kernel projected onto these sources,

$$\int \frac{dx^+ dx^-}{zz'} G_5(j, x-x', z, z') = G_3(j, x_\perp - x'_\perp, z, z') , \quad (4.8)$$

which is precisely the  $AdS_3$  kernel as can be readily seen by integrating Eq. (4.7). The integration measure,  $dx_+ dx_- / (zz')$ , ensures the result is both Lorentz boost and scale invariant. Equivalently this approximation can be stated as restricting the exchanged momentum to the transverse plane, so that  $t = -q_\perp^2$ . Then the  $AdS_5$  momentum-space equation of motion for Pomeron kernel, Eq. (2.15), becomes

$$[-z^5 \partial_z z^{-3} \partial_z + z^2 q_\perp^2 + 2\sqrt{\lambda}(j-2)]\mathcal{K}(j, t, z, z') = (z^5/R^4) \delta(z-z') . \quad (4.9)$$

Merely setting  $q^\pm = 0$  reduces this to the  $AdS_3$  transverse momentum space  $AdS_3$  kernel,  $G_3(j, q_\perp, z, z') = (R^4/zz')\mathcal{K}(j, t, z, z')$ , as it must.

In order to gain a better understanding on the emergence of the  $AdS_3$  algebra, let us discuss the symmetry of the scalar propagator,  $G_3(j, v)$ , in terms of the Euclidean  $AdS_3$  metric,

$$ds^2 = \frac{R^2}{z^2} [dz^2 + dx_1 dx_1 + dx_2 dx_2] = ds^2 = \frac{R^2}{z^2} [dz^2 + dw d\bar{w}] , \quad (4.10)$$

where the transverse subspace is ( $w = x_1 + ix_2, z$ ). The generators of the  $SL(2, C)$  isometries of  $AdS_3$  are

$$\begin{aligned} J_0 &= w \partial_w + \frac{1}{2} z \partial_z , & J_- &= -\partial_w , & J_+ &= w^2 \partial_w + w z \partial_z - z^2 \partial_{\bar{w}} \\ \bar{J}_0 &= \bar{w} \partial_{\bar{w}} + \frac{1}{2} z \partial_z , & \bar{J}_- &= -\partial_{\bar{w}} , & \bar{J}_+ &= \bar{w}^2 \partial_{\bar{w}} + \bar{w} z \partial_z - z^2 \partial_w . \end{aligned} \quad (4.11)$$

In the conformal group, this corresponds to the identification,

$$\begin{aligned} J_0 , J_+ , J_- &\leftrightarrow (-iD + M_{12})/2 , (P_1 + iP_2)/2 , (K_1 - iK_2)/2 \\ \bar{J}_0 , \bar{J}_+ , \bar{J}_- &\leftrightarrow (-iD - M_{12})/2 , (P_1 - iP_2)/2 , (K_1 + iK_2)/2 , \end{aligned}$$

so that the non-zero commutators in  $SL(2, C)$  must be  $[J_0, J_\pm] = \pm J_\pm$ ,  $[J_+, J_-] = 2J_0$ , and  $[\bar{J}_0, \bar{J}_\pm] = \pm \bar{J}_\pm$ ,  $[\bar{J}_+, \bar{J}_-] = 2\bar{J}_0$ . In general, unitary representations of  $SL(2, C)$  are labeled by  $h = i\nu + (1 + n)/2$ , and  $\bar{h} = i\nu + (1 - n)/2$ , which are the eigenvalues for the highest-weight state of  $J_0$  and  $\bar{J}_0$ . The principal series is given by real  $\nu$  and integer  $n$ . The quadratic Casimirs  $J^2$  and  $\bar{J}^2$  have eigenvalues  $h(h - 1)$  and  $\bar{h}(\bar{h} - 1)$  respectively. In the representation (4.11) they are

$$J^2 = J_0^2 + \frac{1}{2}(J_+J_- + J_-J_+) = \frac{1}{4}[z^2\partial_z^2 - z\partial_z + 4z^2\partial_w\partial_{\bar{w}}] \quad (4.12)$$

with  $\bar{J}^2 = \bar{J}_0^2 + \frac{1}{2}(\bar{J}_+\bar{J}_- + \bar{J}_-\bar{J}_+) = \bar{J}^2$  in this representation. (A consequence of  $J^2 = \bar{J}^2$ , for our leading order strong coupling Pomeron, is that we are restricted to  $n = h - \bar{h} = 0$  and are insensitive to rotations in the impact parameter plane by  $M_{12}$ ; we will learn more about this below.) So the boost Hamiltonian  $H_{+-}$  is

$$H_{+-} = 3 - 2J^2 - 2\bar{J}^2 \quad (4.13)$$

expressed in terms of  $SL(2, C)$  Casimirs. This equation realizes the fact that the boost  $M_{+-}$  commutes with all the generators of  $SL(2, C)$  in the conformal group. The quadratic form of the strong-coupling boost operator  $M_{+-}$  then determines the  $J$ -plane eigenvalues to quadratic order in  $\nu$ ,

$$j(\nu) = j_0 - \mathcal{D}\nu^2 + 0(\nu^4) . \quad (4.14)$$

As first pointed out in Ref. [23] the strong coupling BFKL intercept is  $j_0 = 2 - 2/\sqrt{\lambda}$  and the diffusion constant<sup>9</sup> is  $\mathcal{D} = 2/\sqrt{\lambda}$ .

It is interesting to note that this structure is similar to the weak coupling one-loop  $n_g$  gluon BFKL spin chain operator in the large  $N$  limit. Here the boost operator is approximated by  $M_{+-} = 1 - (\alpha N/\pi)H_{\text{BFKL}}$ , where  $H_{\text{BFKL}} = \frac{1}{4} \sum_{i=1}^{n_g} [\mathcal{H}(J_{i,i+1}^2) + \mathcal{H}(\bar{J}_{i,i+1}^2)]$ , a sum over two-body operator with holomorphic and anti-holomorphic functions of the Casimir. The Yang Mills coupling is defined as  $\alpha = g_{YM}^2/4\pi$ . Even numbers of gluons ( $n_g$ ) contribute to the BFKL Pomeron with charge conjugations  $C = +1$  and the odd number of gluons to the so called “odderon” [37, 38, 39, 40, 41] with charge conjugations  $C = -1$ . To be more specific, the operator is defined by its action on two body eigenstates [4, 42, 43],

$$\mathcal{H}(J^2)\Phi_{n,\nu} = \frac{1}{2}[\Psi(h) + \Psi(1 - h) - 2\Psi(1)]\Phi_{n,\nu}. \quad (4.15)$$

---

<sup>9</sup>A cautionary note: in Ref. [23] the integration variable used in solving the Pomeron equation (1.14) is  $2\nu$  and this has the effect that the diffusion constant defined in Ref. [23] is  $\mathcal{D}/4$  compared with the constant defined here.

The symmetry  $h \rightarrow 1 - h$  implies that this is a function of  $h(h - 1)$  or equivalently the quadratic Casimir, which to first order is

$$\mathcal{H}(J^2) + \mathcal{H}(\bar{J}^2) \simeq 2\Psi(\tfrac{1}{2}) - 2\Psi(1) + \frac{1}{2}\Psi''(\tfrac{1}{2})[J^2 + \bar{J}^2 + 1/2] . \quad (4.16)$$

Consequently in the two gluon channel with  $n_g = 2$  and  $H_{\text{BFKL}} = \frac{1}{2}[\mathcal{H}(J_{1,2}^2) + \mathcal{H}(\bar{J}_{1,2}^2)]$ , the leading eigenvalue with  $n = 0$  for the boost is given by

$$j(\nu) = j_0 - \mathcal{D}\nu^2 + 0(\nu^4) , \quad (4.17)$$

with  $j_0 = 1 + 4 \ln 2 \alpha N / \pi$  and  $\mathcal{D} = 14\zeta(3)\alpha N / \pi$ . The two-gluon eigenvectors, written in terms of complex transverse positions  $b_i = x_i + iy_i$  for gluon  $i$ , are

$$\Phi_{n,\nu}(b_1 - b_0, b_2 - b_0) = \left[ \frac{b_1 - b_2}{(b_1 - b_0)(b_2 - b_0)} \right]^{i\nu + (1+n)/2} \left[ \frac{\bar{b}_1 - \bar{b}_2}{(\bar{b}_1 - \bar{b}_0)(\bar{b}_2 - \bar{b}_0)} \right]^{i\nu + (1-n)/2} . \quad (4.18)$$

They are given as a products of conformal and anti-conformal factors with weights  $h = i\nu + (1 + n)/2$  and  $\bar{h} = i\nu + (1 - n)/2$  respectively. Expanding in a Taylor series in  $b_0$  and  $\bar{b}_0$  the wave function is easily seen as a sum of products of infinite-dimensional representations of a two-body Lie algebra. This algebra has  $\vec{J}_{1,2} = \vec{J}^{(1)} + \vec{J}^{(2)}$  represented by  $J_0^{(i)} = b_i \partial_{b_i}$ ,  $J_-^{(i)} = -\partial_{b_i}$ ,  $J_+^{(i)} = b_i^2 \partial_{b_i}$  and similarity for the antiholomorphic sector. In this representation the Casimirs are  $J_{1,2}^2 = -(b_1 - b_2)^2 \partial_{b_1} \partial_{b_2}$  and  $\bar{J}_{1,2}^2 = -(\bar{b}_1 - \bar{b}_2)^2 \partial_{\bar{b}_1} \partial_{\bar{b}_2}$ .

Let us note some differences between the strong-coupling and weakbrained-coupling limits. First,  $j_0$  moves from 1 to 2 as  $\lambda$  moves from small to large. Also, the formulas for  $j(\nu)$  given above have different regimes of validity; at strong coupling the energy-momentum tensor at  $j = 2$  (along with the nearby  $j \sim 2$  DGLAP operators) lies within the region of validity of the strong-coupling expression, while the explicit factor of  $\lambda$  in  $M_{+-}$  at weak coupling implies that Eq. (4.16) breaks down before  $j = 2$ . Also, there is the fact that any  $n$  is allowed at weak-coupling, but we see at strong coupling only  $n = 0$ . Presumably this reflects the nearly point-like nature of a string in this limit, which leaves it unable to undergo rotation in the transverse plane within this approximation. In strong coupling perhaps one should visualize the Pomeron as the exchange of single trace planar diagram with an infinite number of t-channel gluons whose interactions are treated via a mean field approximation.

## 4.2 Pomeron Kernel at High Energies

With the  $J$ -plane Pomeron kernel,  $\mathcal{K}(j, b^\perp, z, z')$ , expressed in terms of the  $AdS_3$  propagator  $G_3(j, v)$ , we would also like to examine the structure of a single Pomeron exchange at high energies,  $\mathcal{K}(s, b^\perp, z, z')$ . This is the kernel which is used in the eikonal resummation, as reviewed in Sec. 3.

Given Eq. (2.17), it follows from Eq. (1.7) that the single Pomeron amplitude can be expressed, after wrapping the  $J$ -plane contour to the left, as

$$\begin{aligned} \mathcal{K}(s, b^\perp, z, z') &= -(zz'/R^4)G_3(j_0, v) \\ &\times \widehat{s}^{j_0} \int_{-\infty}^{j_0} \frac{dj}{\pi} \frac{(1 + e^{-i\pi j})}{\sin \pi j} \widehat{s}^{(j-j_0)} \sin \left[ \xi(v) \sqrt{2\sqrt{\lambda}(j_0 - j)} \right] \end{aligned} \quad (4.19)$$

where we have exposed the dominant BFKL singularity at  $j_0$ . We have also introduced  $\xi(v)$  where  $\cosh \xi = v + 1$ , in order to simplify our expressions.<sup>10</sup>

There are two distinct high energy limits of interest to us: (1)  $\log \widehat{s} \rightarrow \infty$  with  $\sqrt{\lambda}$  large but fixed and (2)  $\log \widehat{s} \rightarrow \infty$ ,  $\lambda \rightarrow \infty$  with  $\log \widehat{s}/\sqrt{\lambda} \rightarrow 0$ . The first is the Regge limit which is dominated by the Pomeron exchange, and the second is dominated by the graviton exchange. Let us give an approximate expression for  $\mathcal{K}$  valid in both these regions.

We begin by separating  $\mathcal{K}$  into its real and imaginary parts,  $\mathcal{K} = \text{Re}[\mathcal{K}] + i\text{Im}[\mathcal{K}]$ ,

$$\begin{aligned} \text{Re}[\mathcal{K}] &= -(zz'/R^4)G_3(j_0, v)\widehat{s}^{j_0} \int_{-\infty}^{j_0} \frac{dj}{\pi} \frac{(1 + \cos \pi j)}{\sin \pi j} \widehat{s}^{j-j_0} \sin \left[ \xi(v) \sqrt{2\sqrt{\lambda}(j_0 - j)} \right] \\ \text{Im}[\mathcal{K}] &= (zz'/R^4)G_3(j_0, v)\widehat{s}^{j_0} \int_{-\infty}^{j_0} \frac{dj}{\pi} \widehat{s}^{j-j_0} \sin \left[ \xi(v) \sqrt{2\sqrt{\lambda}(j_0 - j)} \right]. \end{aligned} \quad (4.20)$$

With the change of integration variable to  $y^2 = 2\sqrt{\lambda}(j_0 - j)$ , the imaginary part is recognized as a Gaussian integral that is easily integrated exactly,

$$\begin{aligned} \text{Im}[\mathcal{K}] &= (zz'/R^4)G_3(j_0, v)\widehat{s}^{j_0} \int_{-\infty}^{\infty} \frac{dy}{2\pi i \sqrt{\lambda}} y e^{-\tau y^2/2\sqrt{\lambda}} e^{i\xi(v)y} \\ &= (zz'/R^4)G_3(j_0, v)(\sqrt{\lambda}/2\pi)^{1/2} \xi e^{j_0\tau} \frac{e^{-\sqrt{\lambda}\xi^2/2\tau}}{\tau^{3/2}}. \end{aligned} \quad (4.21)$$

---

<sup>10</sup>In terms of the new variable  $\xi$ , the combination  $1 + v + \sqrt{v(2+v)} = e^\xi$  and therefore  $G_3(j, v)$  also takes on a simpler form,  $G_3(j, v) = e^{[2-\Delta_+(j)]\xi}/(4\pi \sinh \xi)$ .

The real part is more difficult. However we can find an approximation to  $\text{Re}[\mathcal{K}]$  that is uniformly valid for the region of interest, where both  $\log \hat{s}$  and  $\sqrt{\lambda}$  are large. Large  $\log \hat{s}$  implies that the cut in the  $J$ -plane is probed near the end point for  $j - j_0 < O(1/\log \hat{s})$ . Combined with large  $\sqrt{\lambda}$ , this allows us to expand the prefactor in  $j - 2$ ,

$$\frac{(1 + \cos \pi j)}{\sin \pi j} \simeq \frac{2}{\pi(j - 2)} + O(j - 2) . \quad (4.22)$$

The leading term implies the identity,  $\partial_\tau[e^{-2\tau}\text{Re}[\mathcal{K}]] = -(2/\pi)e^{-2\tau}\text{Im}[\mathcal{K}]$  or an approximation for the real part,

$$\text{Re}[\mathcal{K}] \simeq (zz'/R^4)G_3(j_0, v)(\sqrt{\lambda}/2\pi)^{1/2}\xi \hat{s}^2 \int_\tau^\infty d\tau' \frac{2e^{-2\tau'/\sqrt{\lambda}-\sqrt{\lambda}\xi^2/2\tau'}}{\pi\tau'^{3/2}} . \quad (4.23)$$

Corrections are easily computed in a standard perturbation series. The first order corrections to Eq. (4.23) are  $O(\text{Im}[\mathcal{K}]/\log \hat{s})$  and  $O(\text{Im}[\mathcal{K}]/\sqrt{\lambda})$ , but they are not needed in our present analysis.

Let us first focus on the Regge limit:  $\tau = \log \hat{s} \rightarrow \infty$  at fixed large  $\sqrt{\lambda}$ . In this limit the end point dominates the integral in the expression (4.23) for  $\text{Re}[\mathcal{K}]$  and can be approximated by

$$\int_\tau^\infty d\tau' \frac{2e^{-2\tau'/\sqrt{\lambda}-\sqrt{\lambda}\xi^2/2\tau'}}{\pi\tau'^{3/2}} = (\sqrt{\lambda}/\pi) e^{-2\tau/\sqrt{\lambda}} \frac{e^{-\sqrt{\lambda}\xi^2/2\tau}}{\tau^{3/2}} \left(1 + O(\sqrt{\lambda}/\tau)\right) \quad (4.24)$$

Combining this approximation for  $\text{Re}[\mathcal{K}]$  with  $\text{Im}[\mathcal{K}]$ , we have the leading term in the Regge limit,

$$\mathcal{K} \simeq (zz'/R^4)G_3(j_0, v)e^{j_0\tau} \left[(\sqrt{\lambda}/\pi) + i\right] (\sqrt{\lambda}/2\pi)^{1/2} \xi \frac{e^{-\sqrt{\lambda}\xi^2/2\tau}}{\tau^{3/2}} \quad (4.25)$$

valid for  $\sqrt{\lambda}/\log \hat{s} \rightarrow 0$  and for general value of  $(\sqrt{\lambda}\xi^2)/\log \hat{s}$ . This is our key result. Up to the log factors, the single Pomeron contribution in a transverse representation at high energy is proportional to an  $AdS_3$  propagator at  $j = j_0$  and a diffusion factor in  $\xi$ . This amplitude is complex, with its phase consistent with the Regge signature factor,  $(1 + e^{-i\pi j_0})/2 = (1 + e^{2\pi i/\sqrt{\lambda}})/2 \simeq 1 + i\pi/\sqrt{\lambda}$ , to leading order in  $1/\sqrt{\lambda}$ .

Before discussing in detail the graviton limit, let us make a few additional comments. Let's return to momentum space,

$$\mathcal{K}(s, t, z, z') = \int d^2b^\perp e^{-iq^\perp b^\perp} \mathcal{K}(s, b^\perp, z, z') , \quad (4.26)$$



and examine the high energy behavior at fixed  $t$ . With  $t = -q^{\perp 2} \neq 0$ , one easily verifies that our large  $\widehat{s}$  result,  $\widehat{s}^{j_0}/\log^{3/2}\widehat{s}$  in Eq. (4.25), is consistent with a  $\sqrt{j-j_0}$  BFKL singularity, as derived in [23]. The limit  $t = 0$ , however, requires a more careful treatment. After a more refined analysis, one can verify that Eq. (4.25) leads to Eq. (1.2) and is consistent with the  $1/\sqrt{j-j_0}$  singularity at  $t = 0$  found in Ref. [23].

### 4.3 Connection with Graviton Exchange

Next we turn to the regime dominated by graviton exchange. For  $\lambda \rightarrow \infty$ , the dual theory approaches pure gravity, without stringy corrections. For  $\log \widehat{s} \rightarrow \infty$  and  $\sqrt{\lambda}/\log \widehat{s} \rightarrow \infty$ , the Pomeron exchange should smoothly become graviton exchange. We recall that the amplitude for the one-graviton-exchange Witten diagram in momentum representation, for scalar sources on the boundary of  $AdS_5$ , is [44]

$$\kappa_5^2 \int dz \sqrt{g} \int dz' \sqrt{g'} \tilde{T}^{MN}(p_1, p_3, z) \tilde{G}_{MNM'N'}(q, z, z') \tilde{T}^{M'N'}(p_2, p_4, z') \quad (4.27)$$

where  $\kappa_5$  is the gravitational coupling in  $AdS_5$ ,  $\tilde{T}^{MN}$  is the energy-momentum tensor for the scalar source in the bulk and  $\tilde{G}_{MNM'N'}$  is the graviton propagator, both in momentum representation. At high energies, keeping the leading  $++$ ,  $--$  component, we have shown in Ref. [12] that the corresponding amputated amplitude in transverse representation is

$$\mathcal{K}(s, x^\perp - x'^\perp, z, z') \sim \widehat{s}^2 \left( \frac{zz'}{R^4} \right) G_3(x^\perp - x'^\perp, z, z') \quad (4.28)$$

where  $G_3$  is the dimensionless scalar propagator for a particle of mass  $\sqrt{3}/R$  in an  $AdS_3$  space of curvature radius  $R$ , and in the conformal regime is equal to the function  $G_3(j = 2, v)$  defined in Eq. (1.10). We will now recover this from the Pomeron kernel.

First let us understand where the transition to this regime occurs. For  $\lambda$  sufficiently large, the integral in the expression (4.23) for  $\text{Re}[\mathcal{K}]$  gets its dominant contribution not from the end point at  $\tau$  but at an internal value, at the saddle point determined by  $2\tau'/\sqrt{\lambda} = \sqrt{\lambda}\xi^2/2\tau'$ . The crossover between the Regge and the graviton regimes is determined by the collision of this saddle point with the end point,

$$\xi = 2\tau/\sqrt{\lambda} = (2/\sqrt{\lambda}) \log \widehat{s}. \quad (4.29)$$

To determine the kernel in this regime, let us return to the  $J$ -plane representation, Eq. (4.20), obtained by closing the contour around the BFKL branch point at  $j_0$ . The pole at  $j = 2$  in the integrand, although outside the integration range, plays an increasingly important role in the limit  $\lambda \rightarrow \infty$ . The dominant contribution to the  $J$ -integral now comes from the region  $j = j_0 - 0(1/\sqrt{\lambda})$  and the cutoff for the integral, instead of due to the  $\hat{s}^{(j-j_0)}$  factor, now comes from the last sine factor. In terms of the variable  $y = [2\sqrt{\lambda}(j_0 - j)]^{1/2}$ , the singularity at  $j = 2$  corresponds to poles at  $y = \pm 2i$ .

We first note that, due to the diffusion factor in Eq. (4.21),  $\text{Im}[\mathcal{K}]$  vanishes in this limit. This is not surprising since this  $j = 2$  kinematic singularity does not contribute to  $\text{Im}[\mathcal{K}]$ , (see Eq. (4.20)), and we therefore only need to focus on the real part, which can be expressed as Eq. (4.23). Changing integration variable to  $\tau' = 2\tau/\sqrt{\lambda}$ , the integral in Eq. (4.23) becomes

$$\int_{\tau}^{\infty} d\tau \frac{e^{-2\tau/\sqrt{\lambda} - \sqrt{\lambda}\xi^2/2\tau}}{\tau^{3/2}} = \sqrt{2}\lambda^{-1/4} \int_{2\tau/\sqrt{\lambda}}^{\infty} d\tau' \frac{e^{-\tau' - \xi^2/\tau'}}{\tau'^{3/2}} \quad (4.30)$$

In the limit  $\tau/\sqrt{\lambda} \rightarrow 0$ , the integral yields  $\sqrt{2\pi}\lambda^{-1/4}\xi^{-1}e^{-2\xi}$ , and

$$\mathcal{K} \rightarrow \text{Re}[\mathcal{K}] = \frac{2}{\pi} \hat{s}^2 \left( \frac{zz'}{R^4} \right) G_3(j_0, v) e^{-2\xi(v)} = \frac{2}{\pi} \hat{s}^2 \left( \frac{zz'}{R^4} \right) G_3(2, v) . \quad (4.31)$$

This is the graviton result obtained in Ref. [12], where  $G_3(2, v) \equiv G_3(v)$ , recovered through a  $J$ -plane analysis.

## 5 Aspects of the Eikonal Representation

In this section, we highlight several interesting features of the eikonal approximation for multiple Pomeron exchange. We focus especially on issues of unitarity in the  $s$ -channel, and on the phase of the amplitude, emphasizing its physical interpretation. We also discuss how particle-Pomeron amplitudes are embedded in our calculations, and some connections with the eikonal approximation in flat-space string theory.

Of course the eikonal approximation is commonly used to obtain a manifestly unitary amplitude for a study of unitarity. An S-matrix element which can be approximated by an eikonal sum automatically satisfies the unitarity bound as long as the imaginary part of  $\chi$

is negative. If the eikonal amplitude  $\chi$  for elastic scattering is real, then the eikonal sum precisely saturates the unitarity bound; the elastic amplitude gives the total cross-section. Otherwise, the imaginary part is related to inelastic processes not explicitly described by the elastic amplitude.

Here, the situation is more subtle. We want to compute four-dimensional gauge amplitudes. However, our methods involve the *bulk* eikonal approximation, requiring us to integrate over bulk coordinates,  $z, z'$ , for fixed  $b$ , as in Eq. (3.3). In general, the bulk eikonal approximation is valid in only part of the integration region, the “eikonal region” for short. For this reason, for most values of  $b$ , the gauge-theory amplitude cannot be computed purely within the bulk eikonal approximation, and unitarity of the gauge amplitude cannot be fully studied. Nevertheless, as we will see, unitarity of the bulk amplitude is still conceptually useful and provides some important physical intuition. Later we will consider large values of  $b$  where the eikonal region makes the dominant contribution to the gauge theory amplitude.

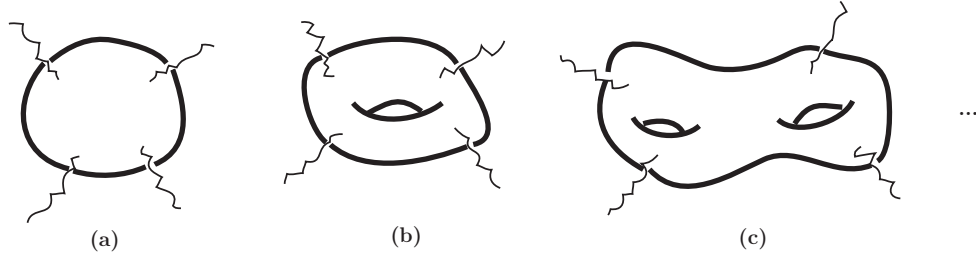


Figure 6: Perturbative expansion for a four-point string amplitude: The planar approximation (a) has  $s$ -channel closed string excitation dual  $t$ -channel complex Regge exchange. The torus diagram (b) has  $s$ -channel threshold for both single closed string excitations and a pairs of closed strings dual to Regge cuts. The two loop diagram gives one, two and three closed string production dual to Regge and multi-Regge cuts, etc.

## 5.1 Inelastic Production and $AdS$

We begin by reviewing familiar aspects of unitarity in four dimensions, and their extension in the present context to physics in the relevant five bulk dimensions.

The unitarity condition for the S matrix,  $S^\dagger S = I$ , can be diagonalized through the  $s$ -channel partial-wave expansion. The  $2 \rightarrow 2$  amplitude can be written

$$A(s, t) = 16\pi \sum_l (2l+1) a_l(s) P_l(\cos \theta), \quad (5.1)$$

where  $a_l(s) \equiv (s_l - 1)/2i$ ,  $s_l \equiv e^{2i\delta_l(s)}$ . The components of the diagonal scattering matrix,  $s_l = e^{2i\delta_l(s)}$ , are unitary for a real phase-shift  $\delta_l(s)$ . In this case elastic scattering in this partial wave saturates unitarity. More generally, if inelastic production is allowed,  $s_l^* s_l < 1$ , and the phase-shift  $\delta_l(s)$  is complex, with  $\text{Im}[\delta_l(s)] > 0$ .

For high-energy small-angle scattering,  $t \simeq -(s/4)\theta^2$ , and with the identification  $l \simeq b\sqrt{s}/2$ , the sum becomes approximately an integral over impact parameter  $b$ , so the partial-wave expansion becomes approximately

$$A(s, t) \simeq -2is \int d^2 b^\perp e^{-iq_\perp b^\perp} (e^{2i\delta(s, b)} - 1) \quad (5.2)$$

For a real phase shift  $\delta(s, b^\perp)$  at high energy, unitarity for the the transverse amplitude,

$$\tilde{A}(s, b^\perp) = \int \frac{d^2 q_\perp}{(2\pi)^2} e^{ib^\perp q_\perp} A(s, t), \quad (5.3)$$

becomes a scalar condition:

$$\text{Im } \tilde{A}(s, b^\perp) = (1/4s) |\tilde{A}(s, b^\perp)|^2. \quad (5.4)$$

In general, at large  $s$ , the on-shell amplitude is an integral of an off-shell position-space Green's function, which depends on the four transverse positions of the two incoming and two outgoing particles. Three of these transverse-position variables are independent; the fourth is removed by translation invariance. In the eikonal approximation, the scattering amplitude at each order in  $\chi$  is proportional to a product of  $\chi$  and two delta functions,  $\delta^2(x_1^\perp - x_3^\perp) \delta^2(x_2^\perp - x_4^\perp)$ , which ensures that neither scattered particle is deflected by a transverse shift in position. This effect of “zero-transverse-deflection” removes two more of the transverse-position variables, leaving an eikonal kernel  $\chi$  that is a function of only one. When the eikonal amplitude is exponentiated, the effect of zero-transverse-deflection is to ensure the full amplitude remains a function of only one transverse position variable. If the eikonal approximation is valid for a given partial wave, that is for a given  $b^\perp$  (at fixed  $s$ ), then the eikonal kernel is nothing but the phase-shift,  $\chi(s, b^\perp) = 2\delta(s, b^\perp)$ . The

general requirements of unitarity on the phase shift  $\delta$ , partial wave by partial wave, thus descend to requirements of unitarity on  $\chi$  which are local in  $b$ . For this reason, we can cease to worry as to whether the eikonal approximation applies to the entire  $S$  matrix; it is enough for us that there are some partial waves to which it applies.

Up to this point we have been discussing standard ideas in four dimensions. Now we turn to the calculation which we have addressed in this paper, which has so far been performed only in conformal four-dimensional field theories (a condition which we will relax later, but which we may retain for now.) Although the conformal theory has no  $S$ -matrix, this is not relevant, since we can add a heavy quark as a probe of the conformal theory and study onium-onium scattering. More important, most gauge theory amplitudes cannot be computed fully within the eikonal approximation; only in some regions of the scattering phase space can it be used. But the eikonal approximation allows us to apply notions of unitarity locally in five dimensions.

To make this statement precise would require a generalization of the notion of partial waves, as in Eq. (5.1), to the bulk. We sidestep this by noting that our form of the amplitude is already a generalization of its high-energy limit Eq. (5.2). Thus we should again view  $\chi(s, b^\perp, z, z')$  as proportional to the phase shift in the high-energy limit of the bulk partial wave expansion,

$$A_{2 \rightarrow 2}(s, t) \simeq \int d^2b \, e^{-ib^\perp q_\perp} \int dz dz' P_{13}(z) P_{24}(z') \tilde{A}(s, b^\perp, z, z') , \quad (5.5)$$

$$\tilde{A}(s, b^\perp, z, z') = -2is \left[ e^{i\chi(s, b^\perp, z, z')} - 1 \right] . \quad (5.6)$$

The key difference between this and the previous case is that the  $z$  coordinate is not translationally invariant, with two important consequences. First, the bulk amplitude in transverse position space is a function of four  $z$  coordinates, which in the eikonal approximation are reduced to two ( $z$  and  $z'$ ), as in Eq. (3.15). Second, the wave functions for the incoming and outgoing particles are not simply plane waves in the  $z$  coordinate, and instead of the simple factor  $e^{-ib^\perp q_\perp}$  which is left over from the wave functions in the Minkowski coordinates, we have the more complicated products of wave functions  $P_{13}(z)P_{24}(z')$ , defined in Eq. (1.5).

Just as the eikonal approximation may not apply in an ordinary four-dimensional scattering amplitude, but may apply in certain partial waves, so here the eikonal approximation will apply only in the limited region we called the “eikonal region”. Where it

does, the full amplitude can be expressed through  $\tilde{A}(s, b^\perp, z, z')$ , a function of one relative Minkowski coordinate and two bulk radial positions, and unitarity applies to it as before.

$$\text{Im } \tilde{A}(s, b^\perp, z, z') \geq (1/4s) |\tilde{A}(s, b^\perp, z, z')|^2. \quad (5.7)$$

A real amplitude  $\chi$ , as for the pure gravity case, saturates the bound, while the complex amplitude of the Pomeron  $\chi$  satisfies a corresponding inequality.

## 5.2 Physical Consequences

We now consider the meaning both of the imaginary part of  $\chi$  and of the imaginary part of  $-2is(e^{i\chi} - 1)$ . Let us expand the eikonal sum in powers of  $\chi$ :

$$\begin{aligned} \text{Im} \tilde{A}(s, b, z, z') &= -2s \text{Re} \left[ \sum_{n=1} (i\chi(s, b, z, z'))^n / n! \right] \\ &= s \{ 2 \text{Im}[\chi(s, b, z, z')] + \text{Re}[\chi^2(s, b, z, z')] + \dots \}. \end{aligned} \quad (5.8)$$

If  $\chi$  is real, as in graviton exchange, contribution to  $\text{Im} \tilde{A}$  begins at one-loop; if  $\chi$  is complex, as for the Pomeron, there is a tree-level contribution.

Whereas the magnitude of the eikonal, (up to log factors), grows as  $G_3(b^\perp, z, z') \hat{s}^{j_0-1}$ , its phase is a *constant*, depending only on  $j_0$ . From Eqs. (3.5) and (4.20),

$$\chi(s, b, z, z') \simeq e^{i(1-j_0/2)\pi} |\chi(s, b^\perp, z, z')|. \quad (5.9)$$

Recall  $j_0$  is the intercept of the leading  $J$ -plane singularity, which moves from  $j_0 \simeq 1$  at weak coupling to  $j_0 \simeq 2$  at strong coupling. This expression requires large energy, so it fails at small  $z, z'$  where the locally measured center-of-mass energy is comparable to or less than the string scale; there the phase goes to zero, for reasons to become clear in a moment.

From the perspective of a  $J$ -plane analysis, an eikonal sum represents an approximate treatment for multi-Pomeron  $J$ -plane singularities, with the  $n$ -loop diagram giving rise to an  $n$ -Pomeron cut at  $j = n(j_0 - 1) + 1$ . For example, the one-loop diagram grows like  $s^{2j_0-1}$  and has a two-Pomeron cut at  $2j_0 - 1$ . Were  $j_0 < 1$ , higher order contributions would be subleading and the eikonal sum would be a rapidly convergent expansion at large  $s$ , but this is not the case for  $1 < j_0 < 2$ , the range of interest here. Therefore,

where the eikonal expansion is reliable, it is interesting to discuss the relative importance of the various perturbative contributions to the absorptive part of the forward amplitude,  $\text{Im}[A(s, 0)]$ , and, thus to the total cross section  $\sigma_{total}(s)$ , through the optical theorem,  $\sigma_{total}(s) \simeq (1/s)\text{Im}[A(s, 0)]$ .

It is important first to elucidate the physical meaning of the phase. In potential theory, elastic scattering dominates when  $\chi$  is real. On the other hand, a black disk (total absorption) gives a pure-imaginary  $\chi$ . A potential with a real and an imaginary part gives a complex  $\chi$ , corresponding to partial absorption.<sup>11</sup> At weak 't Hooft coupling, as in QCD itself, Pomeron exchange corresponds to  $j_0 \rightarrow 1$ , for which  $\text{Re}[\chi] \rightarrow 0$ ; there is nearly complete absorption, and Pomeron exchange approximates a black disk. For graviton exchange,  $j_0 = 2$  and there is no absorption, but at finite large 't Hooft coupling  $j_0 = 2 - 2/\sqrt{\lambda}$  the imaginary part of the tree-level amplitude is nonzero,  $\text{Im}[2\chi] \propto \frac{1}{\sqrt{\lambda}}$ . This absorptive part arises from averaging the effect of massive  $s$ -channel string resonances that arise in the tree-level string amplitude, Fig. 6a. A cut across an exchanged Pomeron looks like a massive string in the  $s$  channel, which gives a pole if  $s$  is equal to the mass of a string; averaging over these poles at large  $s$  gives the Pomeron exchange a nontrivial phase. This inelastic process represents a form of absorption out of the two-string Hilbert space and into the one-string Hilbert space. Other forms of absorption cannot contribute at leading order in the string coupling and at the leading power of  $s$ .<sup>12</sup>

When we move to the one-loop graph, a number of interesting issues arise. On the one hand the imaginary part of the one-loop amplitude is proportional, in the expansion of  $2is[e^{i\chi} - 1]$ , to  $\text{Re}[\chi^2]$ . On the other hand, this same quantity should be given by looking at all the cuts through the one-loop graph, of which there are several. If  $\chi$  is real, as in the exchange of an elementary particle such as a graviton, then the only cut is the obvious one, cutting through both of the scattered particles. This cut is proportional to

---

<sup>11</sup>For a short-range potential with non-vanishing real and imaginary parts,  $V(s, r) = V_R(s, r) - iV_I(s, r)$  the eikonal at high energy is given by

$$\chi(s, b^\perp) = -(2\mu/\sqrt{s}) \int_{-\infty}^{\infty} dz V\left(s, \sqrt{b^{\perp 2} + z^2}\right) \quad (5.10)$$

where  $r^2 = x^2 + y^2 + z^2 = b^{\perp 2} + z^2$  and  $\mu$  is the particle mass. (See, for instance, Schiff, Quantum Mechanics, page: 339-343.)

<sup>12</sup>This type of cut across a large closed string representing, in a confining field theory, a highly excited state that will decay to many hadrons, is called an AGK cut [45, 46].

$\chi^* \chi$ , which is obviously equal to  $\text{Re}[\chi^2]$  in this case.

If  $\chi$  is complex, then one might at first glance add to this first cut two more cuts, one through each Pomeron, which summed together give

$$i\chi \text{Im}[2\chi] + \text{Im}[2\chi](i\chi)^\dagger = -(\text{Im}[2\chi])^2. \quad (5.11)$$

That this is insufficient can be seen by considering the following identity,

$$\begin{aligned} & \text{Re}[\chi(s, b, z, z')\chi(s, b, z, z')] \\ = & \chi^\dagger(s, b, z, z')\chi(s, b, z, z') + i\chi(s, b, z, z')\text{Im}[2\chi(s, b, z, z')] \\ & + \text{Im}[2\chi(s, b, z, z')](i\chi(s, b, z, z'))^\dagger + \frac{1}{2!}(\text{Im}[2\chi(s, b, z, z')])^2 \end{aligned} \quad (5.12)$$

which, from Eq. (5.9), reads

$$\cos(j_0\pi)|\chi|^2 = [1 - 2\sin 2(j_0\pi/2) - 2\sin 2(j_0\pi/2) + 2\sin 2(j_0\pi/2)]|\chi|^2 \quad (5.13)$$

The left hand side is the contribution to  $\text{Im}[\tilde{A}]$  from the second term in  $-ie^{i\chi}$ ; the first (positive) term on the right is the cut through the scattered particles, and the second and third (negative) terms are the cuts through the left and right Pomeron respectively in Fig. 6b. Consistency with Eq. (5.8) requires the last term must be present. It arises in string theory from cutting the torus diagram as one would slice a bagel, with the incoming states on one slice and the outgoing on the other.<sup>13</sup> This positive contribution to the imaginary part corresponds to a new on-shell process not yet included: 2 massive strings propagating in the  $s$ -channel. Only with all four cuts do we obtain the correct second term in Eq. (5.8).<sup>14</sup>

This feature generalizes: for the  $n$ -loop amplitude, one finds  $2^{n+1}$  terms corresponding to up to  $n+1$  strings propagating in the  $s$  channel. In fact all the statements made here for the two-Pomeron exchange graph generalize to all orders, through straightforward combinatorics that build up the exponential.

---

<sup>13</sup>Long ago, in Regge theory, this contribution was identified within field theory. Corresponding to a “Mandelstam diagram” [47, 48], it is the essential mechanism to generate  $j$ -plane cuts from the exchange of two Regge poles.

<sup>14</sup>In string theory there are really only three cuts when viewed topologically, but the first and fourth term above become independent cuts in the limit in which we are working, where we separate massless closed string states in the  $s$ -channel from massive ones. Corresponding subtleties also arise at higher loops. Phenomenologically, this separation identifies “diffractive” vs “non-diffractive” production. Here, diffractive production refers to final states having a large rapidity gap.



It is interesting to compare these features with those arising in the QCD literature regarding the phases in single and multiple Pomeron exchange processes. We have just seen that five-dimensional Pomeron exchange, at leading order, gives a four-dimensional amplitude which is proportional to  $\text{Im}[s^{j_0}]$ , where  $j_0$  is slightly less than 2. QCD data has long been modeled [49] with a similar single four-dimensional Pomeron exchange with  $j_0$  slightly larger than 1. In both cases this poses a problem, since the total cross section, proportional to the imaginary part of the forward amplitude, grows too fast to be consistent with unitarity. In QCD one remedy has been to consider the correction from two-Pomeron exchange, which goes as  $s^{2j_0-1}$ , and whose imaginary part is *negative*, from the left-hand side of Eq. (5.13). This correction therefore gives a negative contribution to the growing single-Pomeron total cross-section. But for  $j_0 > 1.5$ , this picture cannot survive, since the imaginary part of the two-Pomeron exchange correction is positive. Thus, while it is often sufficient at weak coupling to treat the absorptive correction to Pomeron exchange by keeping only the two-Pomeron cut, in strong coupling the totality of the whole eikonal sum must become important.<sup>15</sup>

### 5.3 A Multi-Channel Interpretation

We have, up to now, discussed  $\chi(s, b, z, z')$ , and considered phases and unitarity as applied locally in the bulk. But it is interesting to return to the four-dimensional gauge theory, and to consider what our current discussion means in that context. In particular, in those limited computations where the eikonal region includes the entire bulk, it is possible to reinterpret the bulk eikonal amplitude, a function of  $z$  and  $z'$ , as a field theoretic eikonal amplitude which is a matrix representing transitions between Kaluza-Klein modes. That is, if  $n_1, n_2$  are Kaluza-Klein modes which scatter into modes  $n_3, n_4$ , the amplitude for that transition is a matrix, which is itself the exponential of a matrix eikonal kernel  $\widehat{\chi}$ :

$$-2is \{ \exp [i\widehat{\chi}] - 1 \}_{n_4, n_3; n_2, n_1} \quad (5.14)$$

This represents a multi-channel eikonal approximation, which one could have attempted from the start within quantum field theory. From such a point of view, it would hardly be obvious that the matrix  $\widehat{\chi}$  could be simply diagonalized by representing the modes

---

<sup>15</sup>That the character of diffractive scattering should change as one moves from the region  $j_0 < 1.5$  to  $j_0 > 1.5$  was noted in Ref. [23] in comments relating to black hole production.

labeled by  $n_i$  as functions on a new bulk  $z$  coordinate. In this sense, the gauge-gravity duality performs a small miracle.

Technically, this issue is most easily discussed in the presence of a discrete hadron spectrum, but this requires more formalism than we have presented here. Instead we will simply regulate our conformal field theory with a hard infrared cutoff, which is for many purposes effectively the same thing. We temporarily introduce an IR cut-off in the  $AdS_5$  space,  $0 < z < z_{IR}$ . The  $AdS_5$  spectrum is now discrete, consisting of an infinite sequence of stable KK modes with normalized orthogonal wave functions,  $\Phi^{(n)}(z)$ ,

$$\int_0^{z_{IR}} dz \sqrt{g}(z/R)^2 \Phi^{(n)}(z) \Phi^{(m)}(z) = \delta_{n,m} \quad (5.15)$$

Instead of enumerating them by the co-ordinate  $z \in [0, z_{IR}]$ , we can change basis to the physical on-shell scattering states, using the completeness relation,  $\sum_n \Phi^{(n)}(z) \Phi^{(n)}(z') = (z/R)^3 \delta(z - z')$ . In this basis we have a matrix eikonal expression for all the 2-to-2 on-shell scattering amplitudes,

$$A_{n_4, n_3 \leftarrow n_2, n_1}(s, t) = -2is \int d^2 b e^{-ibq_\perp} [e^{i\hat{\chi}(s, b)} - I]_{n_4, n_3; n_2, n_1}, \quad (5.16)$$

where  $\hat{\chi}$  is a matrix for all possible 2-to-2 scattering amplitudes with a single Regge exchange kernel,

$$\chi_{n_4 n_3; n_2 n_1}(s, b) = \int dz dz' P_{n_3 n_1}(z) P_{n_4 n_2}(z') \chi(s, b, z, z') \quad (5.17)$$

with  $\chi(s, b, z, z')$  given by Eq. (3.5), and  $P_{ij}$  are “overlap functions”, defined in Eq. (1.5). Note that the eikonal matrix is symmetric,  $\chi_{n_4 n_3; n_2 n_1}(s, b) = \chi_{n_2 n_1; n_4 n_3}(s, b)$ . If  $\chi(s, b, z, z')$  is real, the eikonal matrix is hermitian,  $\chi_{n_4 n_3; n_2 n_1}(s, b) = \chi_{n_2 n_1; n_4 n_3}^*(s, b)$ , hence the theory is unitary after incorporating all 2-body inelastic channels made of KK modes. The  $s$ -channel unitarity now takes on a matrix form,

$$\text{Im } A_{n_4 n_3; n_2 n_1}(s, b^\perp) = (1/4s) \sum_{n, m} A^\dagger(s, b^\perp)_{n_4 n_3; nm} A(s, b^\perp)_{nm; n_2 n_1} \quad (5.18)$$

From the field theory point of view, it is remarkable that the scattering matrix of the KK modes can be diagonalized by introducing a single geometric co-ordinate  $z$ . The eikonal amplitude in this basis leads directly back to Eq. (3.3). Indeed, using the orthonormal condition, Eq. (5.15) and the associated completeness relation, one can convert the

multi-channel unitarity condition, Eq. (5.18), into the local unitarity condition, Eq. (5.7), with equality if  $\chi$  is real and inequality if  $\text{Im}\chi > 0$ .

Finally we may let  $z_{IR}$  go to infinity; the modes become continuous but the above relations survive unchanged. Local elastic unitarity remains meaningful when the IR cut-off is removed. In the conformal limit this diagonalization may be viewed a consequence of a conformal partial wave expansion as described in Ref. [43]. However, it is more general, and applies in nonconformal theories.

The multichannel expression in Eq. (5.18) includes the effects of the Kaluza-Klein modes of the bulk graviton, but not those of the higher-mass (and higher-spin) string states. One might hope that this expression can be generalized to include them, and even that the simplicity of the bulk eikonal phase might generalize to the full string theory. While we have not shown this, we will note in Sec. 5.5 that there are interesting and suggestive simplifications in the eikonal approximation to scattering of flat-space strings. It remains to be seen how to incorporate these into a fuller understanding of eikonal scattering of strings in curved space, and whether the difficulties of quantizing strings in Ramond-Ramond backgrounds can be evaded.

## 5.4 Two-Pomeron Cut and Particle-Pomeron Amplitude

The strength of the two-Pomeron cut, which we have evaluated in Sec. 3, can be interpreted as proportional to the square of the “fixed-pole” residue of the particle-Pomeron amplitude. This then provides a connection to the discussion of closed string eikonalization of Ref. [32], which we will turn to in Sec. 5.5, and also allows a generalization of our treatment to include additional corrections such as triple-Pomeron interactions which have been left out of our current analysis.

We have pointed out in Sec. 5.2 that an eikonal sum provides an approximate treatment for the strengths of multi-Pomeron  $J$ -plane singularities. In a  $d = 4$  field theoretic setting, the existence of multi-Pomeron  $J$ -plane singularities was demonstrated by a careful analysis of the analytic structure of non-planar Feynman graphs [47, 48]. This can be generalized to strings through the notion of fixed-pole residues for particle-Pomeron amplitudes. As explained in Sec. 2.2, a fixed-pole residue at  $J = -1$  corresponds to extracting certain spectral weight for an analytic function, e.g., Eq. (2.11). For this residue

not to vanish, the amplitude must satisfy an unsubtracted dispersion relation and has both left- and right-hand cuts.

Recall that in our one-loop analysis in Sec. 3, we are left with two integrals,  $\int dq_1^- A_{13}$  and  $\int dq_1^+ A_{24}$ , where  $A_{13}$  and  $A_{24}$  are particle-Pomeron amplitudes. Let us focus on the integral over  $A_{13}$ , which, in strong coupling, is the a sum of two  $AdS_5$  scalar propagators,  $G_5$ , Fig. 5. As a function of  $M^2 = 2p_1^+ q_1^-$ ,  $A_{13}$  has both a right-hand cut, from the  $s$ -channel propagator, and a left-hand cut, from the  $u$ -channel propagator. It can be represented through a dispersion relation, Eq. (2.6), as the sum of two analytic functions,  $A_{13}(M^2) = A_R(M^2) + A_L(M^2)$ , with a right- and left-hand cut in  $M^2$  respectively. Up to a common factor of  $R^{-3}$ , the first term,  $A_R$ , is  $G_5(M^2)$  and the second,  $A_L$ , is  $G_5(-M^2)$ , where we have suppressed their dependence on transverse coordinates. It can easily be shown that  $G_5(M^2) = 0(1/M^2)$ , whereas the sum  $A_{13}(M^2)$  is even in  $M^2$ , from which we deduce that  $A_{13}(M^2) = 0((1/M^2)^2)$  for  $|M^2| \rightarrow \infty$ .

From the one-loop integral, the path of  $q_1^-$ -integration goes over the  $s$ - and  $u$ -channel physical regions of the amplitude  $A_{13}$ . It leads to an integral in  $M^2$  which goes over the right-hand cut and under the left-hand cut of  $A_{13}(M^2)$ . Since  $A_{13}$  vanishes at infinity as  $0((1/M^2)^2)$ , the integration contour can be freely rotated into the complex  $M^2$  plane, and the integral  $\int dq_1^- A_{13}$ , after multiplying by  $p_1^+/(i\pi)$ , becomes

$$\frac{1}{2\pi i} \int_{-i\infty}^{i\infty} dM^2 A_{13}(M^2) \quad (5.19)$$

Note that the integral is precisely of the form Eq. (2.10), discussed in Sec. 2.2, and it is the  $j = -1$  fixed-pole residue for the particle-Pomeron amplitude,  $A_{13}$ . Here,  $G_5(M^2)$  and  $G_5(-M^2)$  play the role of one-sided analytic functions  $A_R$  and  $A_L$  respectively.

The spectral representation for  $G_5$ , and a completeness relation for Bessel functions, leads to

$$\frac{1}{2\pi i} \int_{-i\infty}^{i\infty} dM^2 A_{13}(M^2) = C_{13} = \delta^2(x_1^\perp - x_3^\perp) (z/R)^3 \delta(z_1 - z_3) \quad (5.20)$$

where we have put back the dependence on transverse coordinates. Together with a similar integral over  $A_{24}$ , it leads to a remarkable result

$$\frac{1}{\pi^2} \int dq_1^- A_{13} \int dq_1^+ A_{24} = (2/s) C_{13} C_{24} = (2/s) (zz'/R^2)^{-2} \langle 3, 4 | 1, 2 \rangle \quad (5.21)$$

from which Eq. (3.14) follows. Since this corresponds to the contribution for the 2-Pomeron cut, we see that the strength of this cut is proportional to the product of two

fixed-pole residues for the respective particle-Pomeron amplitude.

## 5.5 Frozen String Bits in Flat Space

It is interesting to compare our strong coupling results in  $AdS$  space with the eikonal formula of Amati, Ciafaloni and Veneziano [31, 32] for the superstring in flat space. The flat space solution does not require a truncation of the infinite number of normal modes of a full string world sheet description, so similarities with the general mechanism for eikonalization in string theory found in our strong coupling AdS example suggest further generalization beyond strong coupling. In flat space the superstring eikonal phase  $\hat{\chi}$  is a matrix for all 2 to 2 particle scattering amplitudes in the planar approximation. Similarly to our multichannel eikonal amplitude, this matrix can be re-expressed geometrically, this time by a change of basis to an infinite dimensional “impact parameter” space for the transverse positions of individual string “bits”  $x_{\perp}(\sigma)$  of the colliding strings.

Let us review a few of the results of Refs. [31, 32]. Consider the eikonal approximation for graviton-graviton elastic scattering. The first term is the Regge approximation to the planar diagram for graviton scattering,

$$A(s, t) = (\epsilon_3 \cdot \epsilon_1)(\epsilon_4 \cdot \epsilon_2)g_s^2 \mathcal{K}_{\mathcal{P}}(s, q_{\perp}) , \quad (5.22)$$

where  $\epsilon_i$  are the graviton polarization tensors. The kernel for a  $t$ -channel Reggeized graviton exchange is

$$\mathcal{K}_{\mathcal{P}}(s, q_{\perp}) = 2 \frac{\Gamma(1 - \alpha(t)/2)}{\Gamma(\alpha(t)/2)} (e^{-i\pi/2} \alpha' s/4)^{\alpha(t)} , \quad (5.23)$$

where  $t = -q_{\perp}^2$ ,  $\alpha(t) = 2 + \alpha' t/2$ .

As before, the key step for the eikonal approximation of each term in the expansion is well illustrated by the one-loop diagram. In the high-energy small-angle limit, this diagram can be expressed as a box diagram, Fig. 5, with two Pomeron exchange kernels (5.23) for the rungs, coupled to the 2-to-2 Pomeron-graviton scattering amplitudes,  $A_{13}$  and  $A_{24}$ , on the sides of the ladder. Indeed for the flat space superstring, the legitimacy of this approximation has been demonstrated by Sundborg [50] through a detailed analysis of the high energy limit of the exact one loop superstring diagram.

As a result it is proven [31, 32] that the leading two Pomeron cut contribution reduces to the analysis of the Pomeron-particle scattering amplitudes

$$A_{13}(M^2, q_1, q_2) = \int \frac{d^2 z}{\pi} |w|^{-2-\alpha' M^2/2} |1-w|^{\alpha' q_1 q_2} \quad (5.24)$$

on the left side of the ladder, and similarly for  $A_{24}(M'^2, q_1, q_2)$  on the right side, as illustrated in Fig. 4. Here we have defined  $M^2 = -(p_1 + q_1)^2$ ,  $M'^2 = -(p_2 - q_1)^2$  and  $\alpha' q_1 q_2 = \alpha'(t_1 + t_2 - t)/2$ . The box diagram is evaluated by rotating the contour in  $M^2$  for  $A_{13}$  (and in  $M'^2$  for  $A_{24}$ ) in direct analogy with our discussion in Sec. 5.4. Parameterizing the world sheet by  $w = \exp[\tau + i\sigma]$ , the result is

$$C_{13} = \frac{1}{4\pi i} \int_{-i\infty}^{i\infty} dM^2 A_{13}(M^2, q_1, q_2) = \int_0^{2\pi} \frac{d\sigma}{2\pi} |1 - \exp(i\sigma)|^{\alpha' q_1 q_2} \quad (5.25)$$

and similarly  $C_{24}$ . As noted above, these integrals define the residue of the  $J = -1$  fixed pole for a Pomeron-particle scattering amplitude, which sets the strength of the two Pomeron cut at  $2j_0 - 1$ .

Now to make the comparison with our *AdS* eikonal result, it is useful to recast the derivation of Ref. [32] in light-cone gauge [10, 23]. In light-cone gauge, by suitable world-sheet diffeomorphism, the longitudinal modes are fixed so that  $X^+(\sigma, \tau) = \tau$  and  $X^-(\sigma, \tau)$  is dependent on transverse modes via the Virasoro constraint. There are similar conditions on the world sheet fermions, although they don't contribute to the leading eikonal limit. The result is that the transverse coordinates of the string in target space,  $X_\perp(\tau, \sigma)$ , form a complete set of independent bosonic degrees of freedom. One consequence is that the fixed pole integral, Eq. (5.25), demonstrates again that the leading contribution to the eikonal approximation of the one-loop diagram is instantaneous in target space light-cone time:  $x^+ = \tau$ . Moreover, as demonstrated in Ref. [32], this observation holds order by order. For the  $n$ -Pomeron exchange graph, the leading contribution to the  $n$ -Pomeron cut in the  $J$ -plane, which is of order  $(g_s^{2n} s^{n(j_0-1)+1})$ , is instantaneous in  $x^+$ .

Next, following steps similar to our eikonal derivation above, one arrives at the eikonal amplitude [31, 32],

$$T_4(s, t) = -2is(\epsilon_3 \cdot \epsilon_1)(\epsilon_4 \cdot \epsilon_2) \int d^{D-2} b_\perp e^{ib_\perp q^\perp} \langle 0; 0 | [e^{i\hat{\chi}(s, b_\perp; \hat{X}_\perp, \hat{X}'_\perp)} - 1] | 0; 0 \rangle \quad (5.26)$$

with the matrix phase,

$$\hat{\chi}(s, b_{\perp}; \hat{X}_{\perp}, \hat{X}'_{\perp}) = \frac{g_s^2}{2s} \int \frac{d^{D-2}q_{\perp}}{(2\pi)^{D-2}} \mathcal{K}_{\mathcal{P}}(s, q_{\perp}) \int \frac{d\sigma d\sigma'}{(2\pi)^2} e^{iq_{\perp}[b_{\perp} + \hat{X}_{\perp}(\sigma) - \hat{X}'_{\perp}(\sigma')]} . \quad (5.27)$$

The state  $|0; 0\rangle$  is the string vacuum [51] and  $\hat{X}_{\perp}(\sigma)$  are the non-zero mode transverse position operators for the string.<sup>16</sup>

Here we also note that one can exactly diagonalize this matrix by changing basis from the eigenstate of the light-cone string Hamiltonian,

$$P^- = \frac{1}{2p^+} \oint d\sigma [(\hat{\Pi}_{\perp}(\sigma))^2 + \frac{1}{(2\pi\alpha')^2} (\partial_{\sigma} \hat{X}_{\perp}(\sigma))^2] \quad (5.28)$$

to the string bit basis,  $|x_{\perp}(\sigma)\rangle$ , that diagonalizes the transverse position operators  $\hat{X}_{\perp}(\sigma)$ . In light-cone gauge, both bases are a complete representation of all the physical bosonic (non-spurious) modes of the superstring. We change basis for both the right-moving string  $x_{\perp}(\sigma)$  and the left-moving string  $x'_{\perp}(\sigma')$ , obtaining

$$T_4 \sim -2is \int \mathcal{D}x_{\perp} \mathcal{D}x'_{\perp} d^{D-2}b_{\perp} P_{13}[x_{\perp}(\sigma)] P_{24}[x'_{\perp}(\sigma')] e^{ib_{\perp}q^{\perp}} [e^{i\chi(s, b_{\perp}; x_{\perp}, x'_{\perp})} - 1] . \quad (5.29)$$

The string bit probability distributions for flat space string theory

$$P_{31}[x_{\perp}(\sigma)] = |\Phi[x_{\perp}(\sigma)]|^2 \quad \text{and} \quad P_{42}[x'_{\perp}(\sigma')] = |\Phi[x'_{\perp}(\sigma')]|^2 \quad (5.30)$$

are then expressed as the square of Gaussian wavefunctionals [23],

$$\Phi[x_{\perp}(\sigma)] = \langle x_{\perp}(\sigma) | 0; 0 \rangle = \exp\left[-\frac{1}{16\pi^2\alpha'} \oint d\sigma_1 \oint d\sigma_2 \frac{x_{\perp}(\sigma_1)x_{\perp}(\sigma_2)}{\sin^2(\frac{\sigma_1 - \sigma_2}{2}) + \epsilon^2}\right], \quad (5.31)$$

for the overlap of the string vacuum state,  $|0; 0\rangle$ , and the string bit distribution at the time of impact  $x^+ = 0$ . Note that by the state-operator correspondence [51] the graviton wave function also includes a factor  $:\partial X^{\mu}(w)\bar{\partial}X^{\nu}(w)\exp[ipX(w)]:$  at  $|w| = 0$  (or  $\tau = -\infty$ ) but this factor has already been properly included in the spin-momentum factors for each graviton external state in the planar amplitude (5.22).

Thus we see that the geometrical extension of the transverse dimensions that we saw above, where the KK radial mode  $z$  allowed us to rewrite a multi-channel problem

---

<sup>16</sup>At  $|w| = 1$  or  $\tau = 0$ , the zero mode  $\hat{x}_0^{\perp} = \int d\sigma \hat{X}_{\perp}/2\pi$  gives the delta function  $\delta^{D-2}(p_1^{\perp} + p_2^{\perp} + p_3^{\perp} + p_4^{\perp})$ .

in four dimensions using a transverse  $AdS_3$ , has an analogue here. For the string, the exact flat space eikonal amplitude, a multi-channel problem involving a tower of massive string states, is diagonalized using an infinite dimensional space which is a product of transverse impact-parameter spaces, one for each string bit. During the collision, each string bit interacts instantaneously in light-cone time  $X^+ = \tau$  undergoing *zero* deflection. The string bits are frozen.

## 6 Unitarity, Confinement and Froissart Bounds

In this section we address questions relating to unitarity, confinement and the Froissart bound, in regimes where the eikonal approximation in the bulk is believed to give the dominant contribution to the field theory amplitude. If  $b$  is sufficiently large compared to  $z, z'$ , which indicate the sizes (at the moment of collision) of the scattering objects, then the scattering interaction is weak and causes small deflections. In this limit the eikonal approximation is believed in some theories, including gravity, to be a good estimate of the amplitude.

Our discussion below will be brief and we will not consider in detail the effect of the hadron wave functions. Instead we will just discuss the bulk amplitudes at a given  $z$  and  $z'$ . This is a key input for a computation of the full gauge theory amplitude. The wave functions for hadron states peak near a value of  $z$  corresponding to their typical size. The probability that a hadron fluctuates to a smaller size (*i.e.*, is found at smaller  $z$ ) is suppressed by a power law. Meanwhile, the wave functions cut off very quickly at larger  $z$ . Typically the bulk wave functions for hadrons have no support above some maximal  $z$ ; for example all hadrons in a confining theory are cut off at some  $z_{max}$ , and a quarkonium state of mass  $M$  has a wave function with no support for  $z > 1/M$ . Thus, at large  $b$  the properties of the field theory amplitude are to a degree dominated by the properties of the bulk eikonal amplitude at a particular  $z$  and  $z'$ , corresponding to the most likely sizes of the scattering hadrons. However, some of the physics can only be captured after integrating over  $z$  and  $z'$ .

At a given  $z$  and  $z'$ , the cross-section for the partial wave corresponding to  $b$  approaches its unitarity bound when  $|\chi| \sim 1$ . Since interactions become stronger at smaller  $b$ ,  $\partial|\chi|/\partial b$  tends to be negative, so typically the bound is reached for all  $b$  less than some



$b_{max}$ , except possibly for interference fringes. If  $\text{Im}[\chi] > \text{Re}[\chi]$ , as is the case for the weak-coupling Pomeron, the point  $b_{max}$  is where absorption becomes of order one, and one speaks of a black disk of radius  $b_{black}$  where unitarity is saturated. If the reverse is true, as for the strong-coupling Pomeron, then outside the black disk, whose radius is set by  $\text{Im}[\chi] \sim 1$ , is a “diffractive disk”, where one finds large average cross-sections modulated by fringes. The radius of this disk,  $b_{diff}$ , is set roughly by the condition  $\text{Re}[\chi] \sim 1$ . We emphasize however that we are speaking of disks in the bulk, for fixed  $z, z'$ ; the corresponding disks in the gauge theory can be found only by integrating over  $z$  and  $z'$ .

## 6.1 Scattering in the Conformal Case

Within a conformal theory on Minkowski space, there is no S-matrix for the conformal modes themselves, but in the case of a large- $N$  gauge theory we may add heavy quarks, build quarkonium states out of them, and scatter these states off each other. The technique of using “onium-onium” scattering to probe the (near-)conformal part of QCD has a long history [52]. Quarkonium states have been studied in AdS/CFT (see for example [53, 54]) and so this study could be carried out in detail. The calculation would reduce to integrations over  $z$  and  $z'$  of the bulk eikonal formula, weighted by the wave-functions of the onium states.

Preliminary to carrying out such a computation, we will focus some attention on the properties of the bulk eikonal formula  $-2i\hat{s}[e^{i\chi} - 1]$  itself. The parametric dependence of the various physically interesting scales is quite intricate. Their interplay, and the physics for  $\lambda$  closer to 1, deserves further exploration than we will present here.

The kernel is obviously small if  $b$  is much larger than  $z$  and  $z'$ , meaning that the two onium states are far apart compared to their size. Requiring the eikonal phase be of order 1 tells us the radius  $b_{diff}$  where diffraction sets in, for this value of  $z, z'$ . Although the cut in the  $J$ -plane dominates at any fixed  $b, z, z'$  as  $s$  becomes large, the spin-2 exchange dominates at large  $b$  for any fixed  $s, z, z'$ . In Eq. (4.28), we saw that the graviton exchange kernel is proportional to  $G_3(2, v) \sim 1/b^6$  at very large  $b$ . The condition  $\text{Re}[\chi] \sim 1$  determines the radius of the diffractive disk, and if  $\hat{s} = zz's \gg N^2$  and  $b \gg z - z'$  this takes the form:

$$b_{diff} \sim \sqrt{zz'} (zz's/N^2)^{1/6} \quad . \quad (6.1)$$

Since the graviton exchange is real, the disk has diffractive fringes and is non-absorptive. Note however that integrals over  $z$  and  $z'$  will wash out the fringes, giving full absorption. This is interpretable as due to the multi-channel  $2 \rightarrow 2$  process discussed in Sec. 5.3.

At a different radius, the effect of the higher-spin states becomes important and the cut beginning at  $j = j_0$  will dominate over the spin-2 exchange. Here we focus on the regime  $\log s > \sqrt{\lambda}/2$ , which is where long-range effects from the diffusive effect of the Pomeron can become important. The transition between the two regions occurs, from Eq. (4.29), at  $v \sim \hat{s}^{2/\sqrt{\lambda}}$  (where  $v$  is the chordal distance defined in Eq. (1.11),) that is, for  $z \approx z'$ ,

$$b_{\text{cross}} \sim \sqrt{zz'} \sinh \log[(zz's)^{1/\sqrt{\lambda}}] . \quad (6.2)$$

At  $b$  smaller than this,  $\chi$  is determined by Eq. (4.25); its real part now grows slower than  $s^2$  and its imaginary part is nonzero due to  $s$ -channel production of heavy hadrons. We may now ask where  $\text{Im}[\chi] \sim 1$ , using Eq. (4.25). For  $\log s > \sqrt{\lambda}/2$ , this occurs at  $\xi > 1$  and thus  $b/\sqrt{zz'} > 1$ . For  $z = z'$ , the disk may become black at  $b < b_{\text{cross}}$ , in which case

$$b_{\text{black}} \sim \sqrt{zz'} \frac{(zz's)^{(j_0-1)/2}}{\lambda^{1/4}N} , \quad (6.3)$$

an expression which for self-consistency also requires  $s^{j_0-1} > \sqrt{\lambda}N^2$ . But even though the graviton exchange dominates  $\text{Re}[\chi]$  at  $b > b_{\text{cross}}$ , the diffusive tail of the Pomeron can extend into this region and dominate the imaginary part. It is in fact possible that  $b_{\text{black}} > b_{\text{cross}}$ , in which case

$$b_{\text{black}} \sim \sqrt{zz'} \left( \frac{(zz's)^{j_0-1}}{\lambda^{1/4}N} \right)^{1/\sqrt{2\sqrt{\lambda}(j_0-1)}} , \quad (6.4)$$

Again we emphasize that these formulas are at fixed  $z$  and  $z'$  with  $z - z' \ll \sqrt{zz'} < b$ .

Finally, let us recall that the Pomeron kernel is also small if  $z$  and  $z'$  are very different, even if  $b = 0$  (the case of a color-transparent small onium passing through a large one). Requiring the eikonal phase for the Pomeron to be of order 1 gives a condition which (for  $z \ll z'$ ) is approximately

$$(z'/z) \sim (zz's/N^2)^{1/3} , \quad (6.5)$$

where again it is the spin-2 exchange which dominates the result at large  $z'/z$ . Thus for any fixed  $z$  and  $z'$ , saturation takes over from color transparency as  $s$  becomes large. However, here one must treat the hadron wave functions properly to obtain the full picture.

Of course, for these results to be correct, the eikonal approximation must be valid. The approximation breaks down if the scattering angle is too large. In the bulk coordinates this is the requirement that  $\partial\chi/\partial\sqrt{v} \ll \sqrt{\hat{s}}$ . For  $v \gg \hat{s}^{2/\sqrt{\lambda}} \gg 1$  this requires

$$v > \frac{\hat{s}^{1/7}}{N^{4/7}} \quad (6.6)$$

while for  $\hat{s}^{2/\sqrt{\lambda}} \gg v \gg 1$  it requires

$$v > \frac{\hat{s}^{\frac{2}{3}j_0-1}}{N^{4/3}} \quad (6.7)$$

As written these equations are only valid if  $v \sim e^\xi$ , which is only true if  $v \gg 1$ , and thus for self-consistency they require (for  $j_0 \sim 2$ )  $s > N^4$ . For smaller  $s$  the formulas are modified. Note that as  $s$  becomes very large compared to  $N^4$ , the right-hand side is larger than  $b_{\text{black}}$ ; there is no region, for  $\lambda \gg 1$ , where the eikonal approximation is valid and the Pomeron cut is dominant.

We should note that these physical scales in position-space resemble in many ways those found at  $t = 0$  in [33], where deep inelastic scattering and saturation were analyzed. This is because deep inelastic scattering off an onium state, like an onium-onium scattering, probes the conformal regime.

## 6.2 Confinement and the Froissart Bound

Of course there is no Froissart bound in the conformal case because of long-range effects in the conformal gauge theory. If we want to see cross-sections that grow like  $(\log s)^2$  we need to turn to theories with confinement.

With confinement, we can discuss scattering of quarkonia or of ordinary hadrons. We will only touch on a few key points here, leaving a more complete discussion for future work. Also, we only consider here the case where the beta function in the ultraviolet is zero, and the  $J$ -plane has a cut at  $j_0$ ; the physically relevant case of a running coupling adds additional subtleties to an already complex subject.

Although we have spent most of this paper discussing the Pomeron in strictly  $AdS$  space, and our detailed formulas for the kernel (and in particular, their simplicity) depend

on conformal invariance of the dual gauge theory, our methods generalize directly to non-conformal cases. It is completely straightforward to use the  $J$ -plane, and to transform to transverse position space, in the case of non-conformal gauge theories, including confining gauge theories. The problems are purely technical. Unfortunately, few non-conformal cases are known that permit a largely analytic treatment even of the bulk metric. Only one seems approachable, the duality cascade [55], and its small *positive* beta function for the 't Hooft coupling significantly changes the analytic structure in the  $J$ -plane. Moreover, it appears likely that considerable model dependence afflicts the small  $t$  (and therefore large- $b$ ) behavior; also there are some subtleties with identifying leading effects. This potentially means that the various analytically-tractable toy models for confinement, including the hard-wall, D7-metric, and soft-wall models [15, 54, 56, 57], are not reliable here. However, we will still be able to draw some general conclusions.

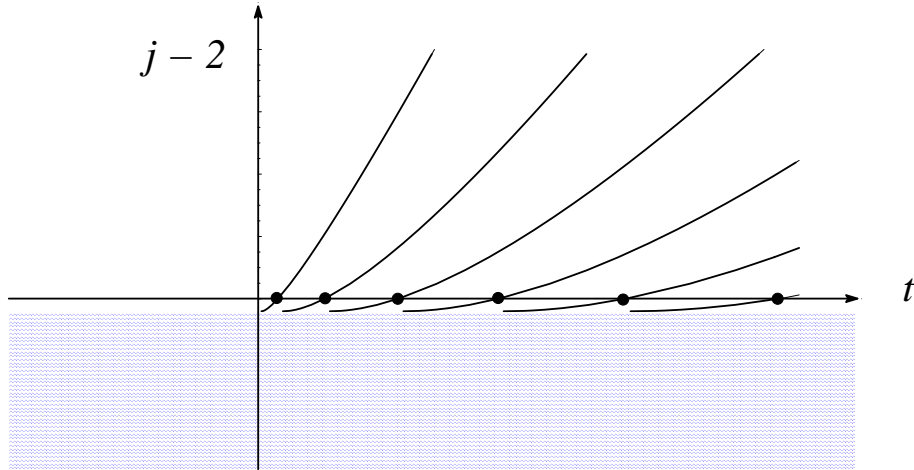


Figure 7: The analytic behavior of Regge trajectories in the hard-wall model, showing the location of the bound-state poles at  $j = 2$  and the  $t$ -independent continuum cut (shaded) at  $j = j_0 = 2 - 2/\sqrt{\lambda}$  into which the Regge trajectories disappear. The lowest Regge trajectory intersects the cut at a small positive value of  $t$ . At sufficiently large  $t$  each trajectory attains a fixed slope, corresponding to the tension of the model's confining flux tubes.

We begin with some general remarks. In a confining theory, the conformal kernel  $\mathcal{K}(j, b^\perp, z, z') = (zz'/R^4)G_3(j, v)$  must be replaced with a more complicated function, one which in a spectral representation should exhibit a sum over discrete states and the

presence of a mass gap in the glueball spectrum. In order to see how new scales can enter with confinement, let us concentrate on the momentum-space Green's function,  $\mathcal{K}(j, t, z, z')$ , which is the two-dimensional Fourier transform of  $\mathcal{K}(j, b^\perp, z, z')$ , and can be obtained as the solution to Eq. (1.16), with  $t = -q_\perp^2$ .

In the conformal limit, the  $J$ -plane consists simply of a single BFKL cut at  $j_0$ . We exhibited this using a spectral representation in  $J$ , Eq. (1.14). Similarly, the lack of a dimensionful scale leads to a continuous spectrum in  $t$  beginning at  $t = 0$ . Using a spectral representation in  $t$ , the kernel is

$$\mathcal{K}(j, t, z, z') = \frac{(zz')^2}{2R^4} \int_0^\infty dk^2 \frac{J_{\tilde{\Delta}(j)}(zk) J_{\tilde{\Delta}(j)}(z'k)}{k^2 - t - i\epsilon} \quad (6.8)$$

where  $\tilde{\Delta}(j) \equiv \Delta_+(j) - 2$ , with  $j > j_0$ . That is,  $\mathcal{K}(j, t, z, z')$  has a branch cut along the positive  $t$ -axis.

Confinement<sup>17</sup> leads to bound states in the  $t$ -channel, with a discrete spectrum [58, 59, 60, 61, 62, 63, 64, 65, 66, 67]. The Green's function is now given by a discrete sum of poles,

$$\mathcal{K}(j, t, z, z') = e^{2A(z)} e^{2A(z')} \sum_{n=0} \frac{\Phi_n(j, z) \Phi_n(j, z')}{t_n(j) - t - i\epsilon}. \quad (6.9)$$

At  $j = 2$ , these poles correspond to an infinite set of spin-two glueballs. We label these discrete modes sequentially,  $n = 0, 1, \dots$ , with the  $t_0(j)$  pole interpolating the lightest spin two glueball.<sup>18</sup> In position space,

$$\mathcal{K}(j, b, z, z') = \frac{1}{2\pi} e^{2A(z)} e^{2A(z')} \sum_{n=0} \Phi_n(j, z) \Phi_n(j, z') K_0(\sqrt{t_n(j)} b). \quad (6.10)$$

Now we would like to understand the properties of  $\mathcal{K}(s, b, z, z')$ , the inverse Mellin transform of the previous formula. We focus on  $z \sim z' \sim z_{max}$ , which gives the largest amplitude for fixed large  $b$ . As in the conformal case, the nearby singularity at  $j = 2$

---

<sup>17</sup>For a confining theory, the five-dimensional metric  $ds^2 = (R/z)^2 dz^2 + e^{-2A(z)} dx^2$  is asymptotically  $AdS_5$  ( $e^{A(z)} \rightarrow z/R$  as  $z \rightarrow 0$ ) and is such that for  $z$  large,  $e^{-2A(z)}$  leads to an effective infrared cutoff,  $z < z_{max}$ . Our main results for the eikonal representation, Eqs. (1.4-1.9), remain valid, after appropriate kinematic modifications due to the confining deformation. All explicit  $z$  and  $z'$  in various prefactors should be replaced by  $Re^{A(z)}$  and  $Re^{A(z')}$  respectively, *e.g.*,  $\hat{s} = zz's$  becomes  $\hat{s} = R^2 e^{A(z)+A(z')} s$ .

<sup>18</sup>For each  $n$ , inverting  $t_n(j)$  leads to a Regge trajectory function,  $\alpha_n(t)$ . Due to a linear confining potential, the trajectory functions are asymptotically linear in  $t$  at large  $j$ .

makes an important contribution at very large  $b$ , for fixed  $s$ . In this case the lightest spin-two glueball, with mass  $m_0 = \sqrt{t_0(2)}$  — makes the most important contribution, falling exponentially as  $e^{-m_0 b}/\sqrt{m_0 b}$ . At much smaller  $b$ , again as in the conformal case, one needs to account for various contributions to the discontinuity across the cut in the  $J$  plane starting at  $j = j_0$ . This cut reflects itself in the above formula in multiple ways. First, the wave functions  $\Phi_n(j, z)$  are singular at  $j = j_0$ , with a square root branch cut of order  $\sqrt{2\sqrt{\lambda}(j - j_0)}$ . That this is true is obvious from the fact that at small  $b, z, z'$  our earlier conformal result must be recovered. Second, the trajectories  $t_n(j)$  will in general have square root branch cuts, also of order  $\sqrt{2\sqrt{\lambda}(j - j_0)}$ .

The hard-wall model, in which the metric is taken to be  $AdS_5$  from  $z = 0$  to  $z = z_{max}$ , and the space is cut off sharply at  $z_{max}$ , illustrates these features. This metric is not a solution to the supergravity equations and has potentially problematic non-analytic behavior at  $z = z_{max}$ , but it does realize confinement and a mass gap, and it is analytically tractable. The complete  $J$ -plane structure of the hard-wall model, as well as the associated kernel, was worked out in [23], and is shown in Fig. 7; note in this model all the Regge trajectories pass below the cut at positive  $t$ . The wave-functions at general  $j$  are Bessel functions,  $\Phi_n(j, z) \sim J_{\tilde{\Delta}(j)}(\sqrt{t_n(j)}z)$ , with the infinite set of discrete modes,  $\{t_n(j)\}$ , determined by boundary conditions at the infrared cutoff  $z_{max}$ . These wave functions pick up a square-root branch cut from the model-independent cut in  $\tilde{\Delta}(j) = \Delta_+(j) - 2$  at  $j = j_0$ ; see Eq. (1.12) for the definition of  $\Delta_+(j)$ . Meanwhile, the basic properties of the branch cuts of  $t_n(j)$  in this model can be inferred from Fig. 9 of [23].

In general, to determine the full form of  $\mathcal{K}(s, b, z, z')$  requires calculating the various contributions to the discontinuity across the cut, and is not trivial. But we also see that all of the branch cuts are of order  $\sqrt{2\sqrt{\lambda}(j - j_0)}$ . For  $z, z'$  held fixed and of order  $z_{max}$ , the integration over  $j - j_0$  will give a diffusion effect in  $b$  of order  $\exp[-c\sqrt{\lambda}b^2m_0^2/\ln s]$ , where  $c$  is a constant of order one that is model-dependent. Thus the diffusive effect in  $b$  space extends only out to a distance proportional to  $(\lambda)^{-1/4}m_0^{-1}$ . The corresponding mass scale is associated with higher-spin hadrons that lie beyond the supergravity regime. Moreover, it appears that the leading trajectory typically has the smallest discontinuity (this is certainly true in the hard wall model) and thus gives the diffusive effect of largest range.

Now let us consider the effect of multiple scattering and unitarization. Since the

effects of the Pomeron cut are short-range, the spin-2 poles dominate the physics at very large  $b$  for fixed  $s$  and  $z, z' \sim z_{max}$  (where the hadron wave functions are largest), with the corrections from higher-spin states only becoming important at shorter range. Thus to understand the behavior of the cross-section, we may focus on the spin-two glueball states. Assuming only the lightest glueball of mass  $m_0$  is important, we find  $|\chi| \sim 1$  inside a radius

$$b_{\text{diff}} \simeq \frac{1}{m_0} \log(s/N^2 \Lambda^2) + \dots \quad (6.11)$$

where  $\Lambda \sim m_0$  is of order the light glueball masses. This approximation is self-consistent; the contribution at this value of  $b$  from the next-to-lightest glueball state becomes relatively small as  $s$  becomes large.

It is important to check whether the eikonal approximation is self-consistent in the regimes we are discussing. A weak but necessary condition is that the scattering causes deflections at small angle, which requires  $b$  be larger than

$$b_{\theta \ll 1} \sim \frac{1}{2m_0} \log(s/N^4 \Lambda^2) + \dots \quad (6.12)$$

The above formula is not quite right, as in this expression we have assumed that only the lightest glueball contributes, which is not true for moderately large  $s$ . But for our immediate purposes, it is enough that the above condition is valid throughout the region where the lightest glueball dominates  $\chi$ , and that the overlap of this region with the region  $|\chi| > 1$  has a large area, proportional to  $(\log[s/N^2 \Lambda^2])^2$ .

In other words, the area in which the scattering amplitude is reaching its unitarity bound, and in which the eikonal scattering is minimally self-consistent, is of order  $(\log s)^2$ . The coefficient of this  $(\log s)^2$  is bounded from above by the inverse mass-squared of the lightest spin-2 glueball, and from below by an unknown (and model-dependent) but nonzero coefficient. This provides strong evidence that the Froissart bound on the total cross-section is not only satisfied, it is saturated.

Of course the eikonal approximation might break down at a radius larger than that given by the above self-consistency condition. But unless this happens right at the edge of the diffractive disk, or our formula for the eikonal phase quickly becomes a large overestimate, the above argument that the Froissart bound is saturated remains intact. Moreover, on physical grounds, any changes to our formulas or breakdown of the eikonal due to so far unidentified effects are unlikely to significantly weaken the scattering amplitude and

bring the amplitude below the unitarity bound in any of the region  $b < b_{\text{diff}}$ ; in fact, the interactions being gravitational, they are likely to make the scattering amplitude larger. Thus our conclusion appears robust.<sup>19</sup>

## 7 Summary and Outlook

In this paper, we have taken a step toward unitarization of high energy scattering using string/gauge duality. The eikonal approximation is a summation to all orders (in  $1/N^2$ , or  $g_s$ ) of multiple small-angle scatterings. Here we have computed scattering amplitudes (or partial contributions to scattering amplitudes) in large- $\lambda$  gauge theories by using the eikonal approximation for multiple Pomeron exchange. We have seen the required formalism is a relatively straightforward generalization of our approach to multiple graviton exchange in  $AdS_5$  space. All we needed to do was convert our earlier work on the Pomeron [18, 23] from momentum space to transverse position space, use a  $J$ -plane representation of the amplitude, and combine it with the techniques of [12].

We carried this program out in its entirety in the case of a conformal field theory, where the symmetries of the problem make it easy to solve. We showed that in transverse position space and the  $J$ -plane, the Pomeron exchange amplitude is extremely simple: it is proportional to a scalar  $AdS_3$  propagator. We examined the group-theoretic basis of this result, comparing it to known results at weak coupling. We noted that the Pomeron cut dominates as  $s$  goes to infinity for fixed  $\lambda$ , and recovered a graviton-exchange kernel by holding  $s$  fixed and letting  $\lambda$  grow to infinity. The eikonalization of this amplitude also had a number of interesting features which we highlighted: a nontrivial phase compared to the graviton, corresponding to production in the  $s$ -channel of excited strings; a multi-channel interpretation; and a string-bit interpretation. These multiple viewpoints will be useful for the next steps in the conformal case: corrections to the one-Pomeron exchange approximation to the eikonal kernel from triple-Pomeron vertices, and corrections beyond

---

<sup>19</sup>We note that the proposal of Giddings on the role of black holes and the Froissart bound [9, 68, 69] suggests but does not strictly prove a lower bound. Because of the difficulty of computing the rate of black-hole production and the efficiency with which the initial energy is converted to black hole mass, it is not clear to us whether the lower-bound obtained from black hole production would be larger or smaller than the one we are discussing here. Note also that because there might be other processes with larger cross-sections, Giddings suggestion provides no upper bound.



the eikonal approximation. A further goal is a complete Gribov-Regge effective theory in the large- $\lambda$  limit.

We finally turned to issues of unitarity in a bit more detail. We first considered how the Pomeron appears within the bulk amplitude in the conformal case, noting where the graviton exchange contribution takes over. We also considered issues of color transparency and the onset of saturation. We then turned our attention to confining theories. Here we found unitarity saturated in a disk with radius growing like  $\log s$ , given by multiple exchange of light spin-two glueballs. Within the eikonal approximation, it appears that the Froissart bound is not only satisfied in the generic large- $\lambda$  theory, it is also saturated. To establish lower as well as upper bounds on the cross-section in any given theory will require more careful analysis.

In future, it will be important to compute a variety of scattering amplitudes and interpret the results; [33] has recently begun this program in the context of deep-inelastic scattering. Eventually one would hope to extract appropriate lessons for QCD, though this will be a challenge, given the intricate dependence of the physics on  $s$ ,  $b$ ,  $\lambda$  and  $N$ . In particular, the approach to the region  $\lambda \rightarrow 1$  holds some subtleties that are yet to be explored.

Acknowledgments: We are pleased to acknowledge useful conversations with D. Freedman, M. H. Fried, A. Kovner, J. Polchinski, and G. Veneziano. The work of R.C.B. was supported by the Department of Energy under Contract. No. DE-FG02-91ER40676, that of M.J.S. by U.S. Department of Energy Contract. No. DE-FG02-96ER40956 and that of C-I.T. was supported by the Department of Energy under Contract No. DE-FG02-91ER40688, Task-A. C-I.T. and R.C.B. would like to thank the Aspen Center for Physics for its hospitality during the writing of this paper. We are grateful to the Benasque Center for Science, where this work was initiated.

## References

- [1] G. F. Chew and S. C. Frautschi, “Principle of Equivalence for All Strongly Interacting Particles within the S Matrix Framework,” *Phys. Rev. Lett.* **7** (1961) 394–397.
- [2] V. N. Gribov, “Partial waves with complex orbital angular momenta and the asymptotic behavior of the scattering amplitude,” *Sov. Phys. JETP* **14** (1962) 1395.
- [3] L. N. Lipatov, “Reggeization of the Vector Meson and the Vacuum Singularity in Nonabelian Gauge Theories,” *Sov. J. Nucl. Phys.* **23** (1976) 338–345.
- [4] E. A. Kuraev, L. N. Lipatov, and V. S. Fadin, “The Pomeron Singularity in Nonabelian Gauge Theories,” *Sov. Phys. JETP* **45** (1977) 199–204.
- [5] I. I. Balitsky and L. N. Lipatov, “The Pomeron Singularity in Quantum Chromodynamics,” *Sov. J. Nucl. Phys.* **28** (1978) 822–829.
- [6] A. Capella, J. Tran Thanh Van, U. Sukhatme, and C. I. Tan, “The Pomeron Story.” in *A Passion For Physics*, World Scientific (1984), 79–87.
- [7] A. Donnachie and P. V. Landshoff, “Total Cross-Sections,” *Phys. Lett.* **B296** (1992) 227–232, [hep-ph/9209205](#).
- [8] G. F. Giudice, R. Rattazzi, and J. D. Wells, “Transplanckian collisions at the LHC and beyond,” *Nucl. Phys.* **B630** (2002) 293–325, [hep-ph/0112161](#).
- [9] S. B. Giddings, “High energy QCD Scattering, the Shape of Gravity on an IR Brane, and the Froissart Bound,” *Phys. Rev.* **D67** (2003) 126001, [hep-th/0203004](#).
- [10] S. B. Giddings, D. J. Gross, and A. Maharana, “Gravitational effects in ultrahigh-energy string scattering,” [arXiv:0705.1816 \[hep-th\]](#).
- [11] L. Cornalba, M. S. Costa, and J. Penedones, “Eikonal Approximation in AdS/CFT: Resumming the Gravitational Loop Expansion,” [arXiv:0707.0120 \[hep-th\]](#).
- [12] R. C. Brower, M. J. Strassler, and C.-I. Tan, “On the Eikonal Approximation in AdS Space,” [arXiv:0707.2408 \[hep-th\]](#).

- [13] L. Cornalba, M. S. Costa, J. Penedones, and R. Schiappa, “Eikonal approximation in AdS/CFT: From shock waves to four-point functions,” [hep-th/0611122](#).
- [14] L. Cornalba, M. S. Costa, J. Penedones, and R. Schiappa, “Eikonal approximation in AdS/CFT: Conformal partial waves and finite n four-point functions,” *Nucl. Phys.* **B767** (2007) 327–351, [hep-th/0611123](#).
- [15] J. Polchinski and M. J. Strassler, “Hard scattering and gauge/string duality,” *Phys. Rev. Lett.* **88** (2002) 031601, [hep-th/0109174](#).
- [16] R. C. Brower and C.-I. Tan, “Hard Scattering in the M-Theory Dual for the QCD String,” *Nucl. Phys.* **B662** (2003) 393–405, [hep-th/0207144](#).
- [17] S. J. Brodsky and G. F. de Teramond, “Light-Front Hadron Dynamics and AdS/CFT Correspondence,” *Phys. Lett.* **B582** (2004) 211–221, [hep-th/0310227](#).
- [18] J. Polchinski and M. J. Strassler, “Deep inelastic scattering and gauge/string duality,” *JHEP* **05** (2003) 012, [hep-th/0209211](#).
- [19] R. A. Janik and R. Peschanski, “High Energy Scattering and the AdS/CFT Correspondence,” *Nucl. Phys.* **B565** (2000) 193–209, [hep-th/9907177](#).
- [20] R. A. Janik, “String Fluctuations, AdS/CFT and the Soft Pomeron Intercept,” *Phys. Lett.* **B500** (2001) 118–124, [hep-th/0010069](#).
- [21] O. Andreev and W. Siegel, “Quantized Tension: Stringy Amplitudes with Regge Poles and Parton Behavior,” *Phys. Rev.* **D71** (2005) 086001, [hep-th/0410131](#).
- [22] H. Nastase, “The soft pomeron from AdS-CFT,” [hep-th/0501039](#).
- [23] R. C. Brower, J. Polchinski, M. J. Strassler, and C.-I. Tan, “The Pomeron and Gauge / String Duality,” [hep-th/0603115](#).
- [24] E. Levin and C.-I. Tan, “Heterotic Pomeron: A Unified Treatment of High-Energy Hadronic Collisions in QCD,” [hep-ph/9302308](#).
- [25] S. Bondarenko, E. Levin, and C. I. Tan, “High Energy Amplitude as an Admixture of Soft and Hard Pomerons,” *Nucl. Phys.* **A732** (2004) 73, [hep-ph/0306231](#).

- [26] T. Jaroszewicz, “Gluonic Regge Singularities and Anomalous Dimensions in QCD,” *Phys. Lett.* **B116** (1982) 291.
- [27] L. N. Lipatov, “Small- $x$  Physics in Perturbative QCD,” *Phys. Rept.* **286** (1997) 131–198, [hep-ph/9610276](#).
- [28] A. V. Kotikov and L. N. Lipatov, “NLO Corrections to the BFKL Equation in QCD and in Supersymmetric Gauge Theories,” *Nucl. Phys.* **B582** (2000) 19–43, [hep-ph/0004008](#).
- [29] A. V. Kotikov and L. N. Lipatov, “DGLAP and BFKL Equations in the  $\mathcal{N} = 4$  Supersymmetric Gauge Theory,” *Nucl. Phys.* **B661** (2003) 19–61, [hep-ph/0208220](#).
- [30] A. V. Kotikov, L. N. Lipatov, A. I. Onishchenko, and V. N. Velizhanin, “Three-Loop Universal Anomalous Dimension of the Wilson Operators in  $\mathcal{N} = 4$  SUSY Yang-Mills Model,” [hep-th/0404092v5](#).
- [31] D. Amati, M. Ciafaloni, and G. Veneziano, “Superstring Collisions at Planckian Energies,” *Phys. Lett.* **B197** (1987) 81.
- [32] D. Amati, M. Ciafaloni, and G. Veneziano, “Classical and quantum gravity effects from Planckian energy superstring collisions,” *Int. J. Mod. Phys.* **A3** (1988) 1615–1661.
- [33] Y. Hatta, E. Iancu, and A. H. Mueller, “Deep inelastic scattering at strong coupling from gauge/string duality : the saturation line,” [arXiv:0710.2148](#) [[hep-th](#)].
- [34] R. C. Brower, C. E. DeTar, and J. H. Weis, “Regge Theory for Multiparticle Amplitudes,” *Phys. Rept.* **14** (1974) 257.
- [35] H. Cheng and T. T. Wu, “Impact factor and exponentiation in high-energy scattering processes,” *Phys. Rev.* **D186** (1969) 1611–1618.
- [36] S.-J. Chang and T.-M. Yan, “High-energy elastic and inelastic scattering in phi-to-the- third theory,” *Phys. Rev.* **D4** (1971) 537–558.
- [37] L. Lukaszuk and B. Nicolescu, “A Possible Interpretation of p p Rising Total Cross-Sections,” *Nuovo Cim. Lett.* **8** (1973) 405–413.

- [38] G. Bialkowski, K. Kang, and B. Nicolescu, “High-Energy Data and the Structure of the Odd Signature Amplitude of Pion-Nucleon Scattering,” *Nuovo Cim. Lett.* **13** (1975) 401.
- [39] J. Kwiecinski and M. Praszalowicz, “Three Gluon Integral Equation and Odd C Singlet Regge Singularities in QCD,” *Phys. Lett.* **B94** (1980) 413.
- [40] J. Finkelstein, H. M. Fried, K. Kang, and C. I. Tan, “Forward Scattering at Collider Energies and Eikonal Unitarization of Odderon,” *Phys. Lett.* **B232** (1989) 257.
- [41] J. Bartels, L. N. Lipatov, and G. P. Vacca, “A New Odderon Solution in Perturbative QCD,” *Phys. Lett.* **B477** (2000) 178–186, [hep-ph/9912423](#).
- [42] L. N. Lipatov, “The Bare Pomeron in Quantum Chromodynamics,” *Sov. Phys. JETP* **63** (1986) 904–912.
- [43] V. M. Braun, G. P. Korchemsky, and D. Mueller, “The uses of conformal symmetry in QCD,” *Prog. Part. Nucl. Phys.* **51** (2003) 311–398, [hep-ph/0306057](#).
- [44] E. D’Hoker, D. Z. Freedman, S. D. Mathur, A. Matusis, and L. Rastelli, “Graviton exchange and complete 4-point functions in the AdS/CFT correspondence,” *Nucl. Phys.* **B562** (1999) 353–394, [hep-th/9903196](#).
- [45] V. A. Abramovskii, O. V. Kancheli, and V. N. Gribov, “Structure of inclusive Spectra and Fluctuations in Inelastic Processes Caused by Multiple-Pomeron Exchange,” *eConf* **C720906V1** (1972) 389–413.
- [46] V. A. Abramovsky, V. N. Gribov, and O. V. Kancheli, “Character of Inclusive Spectra and Fluctuations Produced in Inelastic Processes by Multi-Pomeron Exchange,” *Yad. Fiz.* **18** (1973) 595–616.
- [47] S. Mandelstam, “Cuts in the Angular Momentum Plane. 1,” *Nuovo Cim.* **30** (1963) 1128.
- [48] S. Mandelstam, “Cuts in the Angular Momentum Plane. 2,” *Nuovo Cim.* **30** (1963) 1148–1162.
- [49] A. Capella, U. Sukhatme, C.-I. Tan, and J. Tran Thanh Van, “Dual parton model,” *Phys. Rept.* **236** (1994) 225–329.

- [50] B. Sundborg, “High-energy asymptotics: The one loop string amplitude and resummation,” *Nucl. Phys.* **B306** (1988) 545–566.
- [51] J. Polchinski, “String Theory. Vol. 1: An Introduction to the Bosonic String,” Cambridge, UK: Univ. Pr. (1998) 402 p.
- [52] A. H. Mueller, “Unitarity and the BFKL Pomeron,” *Nucl. Phys.* **B437** (1995) 107–126, [hep-ph/9408245](#).
- [53] A. Karch and E. Katz, “Adding Flavor to AdS/CFT,” *JHEP* **06** (2002) 043, [hep-th/0205236](#).
- [54] M. Kruczenski, D. Mateos, R. C. Myers, and D. J. Winters, “Meson spectroscopy in AdS/CFT with Flavour,” *JHEP* **07** (2003) 049, [hep-th/0304032](#).
- [55] I. R. Klebanov and M. J. Strassler, “Supergravity and a Confining Gauge Theory: Duality Cascades and  $\chi$ SB-Resolution of Naked Singularities,” *JHEP* **08** (2000) 052, [hep-th/0007191](#).
- [56] D. T. Son and M. A. Stephanov, “QCD and Dimensional Deconstruction,” *Phys. Rev.* **D69** (2004) 065020, [hep-ph/0304182](#).
- [57] A. Karch, E. Katz, D. T. Son, and M. A. Stephanov, “Linear Confinement and AdS/QCD,” *Phys. Rev.* **D74** (2006) 015005, [hep-ph/0602229](#).
- [58] E. Witten, “Anti-de Sitter Space and Holography,” *Adv. Theor. Math. Phys.* **2** (1998) 253–291, [hep-th/9802150](#).
- [59] C. Csaki, H. Ooguri, Y. Oz, and J. Terning, “Glueball Mass Spectrum from Supergravity,” *JHEP* **01** (1999) 017, [hep-th/9806021](#).
- [60] R. de Mello Koch, A. Jevicki, M. Mihailescu, and J. P. Nunes, “Evaluation of Glueball Masses from Supergravity,” *Phys. Rev.* **D58** (1998) 105009, [hep-th/9806125](#).
- [61] O. Aharony, S. S. Gubser, J. M. Maldacena, H. Ooguri, and Y. Oz, “Large  $N$  Field Theories, String Theory and Gravity,” *Phys. Rept.* **323** (2000) 183–386, [hep-th/9905111](#).

- [62] N. R. Constable and R. C. Myers, “Spin-two Glueballs, Positive Energy Theorems and the AdS/CFT Correspondence,” *JHEP* **10** (1999) 037, [hep-th/9908175](#).
- [63] R. C. Brower, S. D. Mathur, and C.-I. Tan, “Discrete Spectrum of the Graviton in the AdS(5) Black Hole Background,” *Nucl. Phys.* **B574** (2000) 219–244, [hep-th/9908196](#).
- [64] R. C. Brower, S. D. Mathur, and C.-I. Tan, “Glueball Spectrum for QCD from AdS Supergravity Duality,” *Nucl. Phys.* **B587** (2000) 249–276, [hep-th/0003115](#).
- [65] L. A. Pando Zayas, J. Sonnenschein, and D. Vaman, “Regge Trajectories Revisited in the Gauge / String Correspondence,” *Nucl. Phys.* **B682** (2004) 3–44, [hep-th/0311190](#).
- [66] E. Caceres and C. Nunez, “Glueballs of Super Yang-Mills from Wrapped Branes,” *JHEP* **09** (2005) 027, [hep-th/0506051](#).
- [67] H. Boschi-Filho, N. R. F. Braga, and H. L. Carrion, “Glueball Regge Trajectories from Gauge/String Duality and the Pomeron,” [hep-th/0507063](#).
- [68] K. Kang and H. Nastase, “High energy QCD from planckian scattering in AdS and the froissart bound,” *Phys. Rev.* **D72** (2005) 106003, [hep-th/0410173](#).
- [69] K. Kang and H. Nastase, “Heisenberg saturation of the froissart bound from AdS-CFT,” *Phys. Lett.* **B624** (2005) 125–134, [hep-th/0501038](#).